Grant DE-FG02-04ER83890
DOE Ref. Number DOE/ER/83890-1
ARI Project 10366
ARI Report RR-1460

Development of Soft Ionization for Particulate Organic Detection with the Aerodyne Aerosol Mass Spectrometer

Final Report
July 11, 2005 –January 10, 2008

Prepared by

A. Trimborn, L.R. Williams, J.T. Jayne, D.R. Worsnop
Center for Aerosol and Cloud Chemistry
Aerodyne Research, Inc.
45 Manning Road
Billerica, MA 01821

Prepared for
Richard C. Petty
U.S. Department of Energy
SC-23.3 / Germantown Building
1000 Independence Avenue, S.W.
Washington, DC 20585-1290

Development of Soft Ionization for Particulate Organic Detection with the Aerodyne Aerosol Mass Spectrometer

Executive Summary

In this DoE-supported SBIR Phase II project, we have developed several soft ionization techniques for use with the Aerodyne Aerosol Mass Spectrometer (AMS). The AMS allows quantitative, real-time, size and composition analysis of atmospheric aerosol particles [*Jayne et al.*, 2000]. AMS measurements of aerosol chemistry are routine and are now standard in most field campaigns, including those supported by DoE as well as other agencies (worldwide) [*Canagaratna et al.*, 2007; *Zhang et al.*, 2007]. This work has recently been highlighted in *Science* [*Robinson et al.*, 2007] which used laboratory and field AMS results to estimate regional secondary organic aerosol (SOA) budgets. That work drew heavily on DoE-supported AMS results from Mexico City in 2003 [*Volkamer et al.*, 2006] that showed that photochemical SOA production occurs daily on a time scale of hours in Mexico City. Additionally, the AMS is now routinely used in chamber studies of the chemistry of SOA formation, allowing for the chemical characterization of laboratory-generated organic aerosol [*Bahreini et al.*, 2005; *Alfarra et al.*, 2006]. Recently we have developed a time-of-flight mass spectrometer version of the AMS (ToF-AMS), leading to substantial increases in the sensitivity, resolution, and data acquisition rate of the instrument [*Drewnick et al.*, 2005; *DeCarlo et al.*, 2006]. This development, which included significant DoE support, has led to the deployment of over 20 ToF-AMS systems worldwide, including two in DoE laboratories, and deployment on the DoE G-1 aircraft.

The goal of this project is to enhance the molecular information that can be derived from aerosol mass spectra. The standard mode of AMS operation involves ionization by electron impact (EI), which is a proven, quantitative technique, but involves the extensive fragmentation of individual ions, making the identification and characterization of individual organics in the aerosol rather difficult. During this DOE SBIR Phase II project, we have developed several soft ionization techniques, i.e., ionization schemes which involve less fragmentation of the ions, for use with the ToF-AMS. This SBIR program has successfully accomplished the tasks in the Phase II proposal, including:

1. Vacuum ultraviolet single photon ionization was demonstrated in the laboratory and deployed in field campaigns [*Northway et al.*, 2007]. This demonstration has led to collaboration with a German group [*Mühlberger et al.*, 2005b] to continue VUV lamp development undertaken by the University of Colorado during the SBIR.
2. Dissociative electron attachment is also now a routine approach with AMS systems configured for bipolar, negative ion detection. This technique is particularly powerful for detection of acidic and other highly oxygenated SOA chemical functionality.
3. Low energy electron ionization is now a "softer" ionization approach routinely available to AMS users.
4. Lithium ion (Li^+) attachment has been shown to be sensitive to more alkyl-like chemical functionality in SOA. Results from Mexico City are particularly exciting in observing changes in SOA molecular composition under different photochemical/meteorological conditions. More recent results detecting biomass burns at the Montana fire lab have demonstrated quantitative and selective detection of levoglucosan, for example.

Introduction

Organic aerosols are well known to affect human health [*Dockery et al.,* 1993], visibility [*Watson*, 2002], agriculture, and climate [*IPCC*, 2007]. Organic aerosols compose up to 50% of all fine particulate matter below 2.5 μm (PM 2.5) in urban areas and under many circumstances organic material may account for the majority of the ambient aerosol mass [*Kalberer et al.*, 2004]. It is now widely surmised that organic aerosols contain up to hundreds of organic compounds in many chemical classes including alkanes, aldehydes, aromatics, acids and polymers [*Kalberer et al.*, 2004; *IPCC*, 2007]. Of this organic aerosol mass, only a small fraction has been compositionally resolved, and much of the organic aerosol mass remains uncharacterized to this date. This lack of knowledge represents a large uncertainty in the role of anthropogenic activities on the future climate and on human health effects.

In view of the complexity of atmospheric aerosol chemistry, there is a real need for new approaches to the aerosol characterization problem, in particular for organic compounds [*Murphy*, 2005]. Aerosol mass spectrometry is a growing area of focus for aerosol speciation because of the wealth of information it can provide on a wide variety of chemical classes in real time. Aerosol mass spectrometers generally detect particles through either a single-step particle vaporization/ionization process (laser ablation) [*Murphy et al.*, 1998; *Noble and Prather*, 2000] or a two-step vaporization/ionization process using a combination of laser desorption/thermal vaporization and various ion detection methods [*Jayne et al.*, 2000; *Woods et al.*, 2001]. The mass spectra of ambient aerosol (particularly organic aerosol) obtained with these instruments are generally complex due to the extensive fragmentation caused by the high-energy ionization methods they use.

The Aerodyne Aerosol Mass Spectrometer (AMS) is widely used for obtaining both quantitative chemical composition and size information for aerosols in real-time with no need for pre-concentration of samples [*Woods et al.*, 2001; *Canagaratna et al.*, 2007]. The standard instrument uses a combination of flash vaporization, electron impact ionization, and quadrupole or time-of-flight mass spectrometry to detect fragment ions of the non-refractory component of aerosol particles. Since 70 eV electron impact is universal and inherently linear, it provides the AMS with quantification and broad detection capabilities. A drawback of the combined flash vaporization and EI ionization detection scheme of the AMS is that it results in extensive fragmentation of organic ions and limits its organic speciation capability. A deconvolution technique has been developed recently to estimate the mass concentrations and size distributions of hydrocarbon-like and oxidized organic aerosols in ambient air using the spectral signatures of m/z 57 and m/z 44 as "first order" tracers for fresh "hydrocarbon-like" and oxygenated organic aerosols, respectively [*Zhang et al.*, 2005]. Since organic aerosols consist of hundreds of individual chemical species, however, more specific information about the organic species in the aerosol is of great interest.

Soft Ionization with Vacuum Ultraviolet (VUV) Photons

Less energetic, "soft" ionization methods, such as single photon ionization (SPI) with vacuum ultraviolet (VUV) energy have been shown to simplify the complexity of organic mass spectra in both gas-phase and aerosol phase mixtures [*Butcher et al.*, 1999; *Mühlberger et al.*, 2002; *Sykes et al.*, 2002; *Oktem et al.*, 2004]. Resonance-enhanced multi photon ionization (REMPI) is a related soft ionization technique that is highly sensitive, but generally suitable only for (UV absorbing) aromatic components of organic aerosol [*Heger et al.*, 1999; *Mühlberger et al.*, 2001; *Cao et al.*, 2003]. Single photon ionization is a more quantitative and linear technique

and therefore is more promising for the analysis of gaseous species from the thermal vaporization of aerosol beams. The use of relatively complex laser systems for the production of pulsed VUV light, in many of these experiments, however, complicates the deployment of using these instruments in the field.

Recently, several new sources of VUV radiation have been developed as alternatives to lasers. Low-pressure lamps filled with noble gases provide continuous sources of VUV photons that may be used to ionize a vapor plume of organic molecules. Nearly all of the organic compounds have ionization energy bands lying within the energy range 8-11 eV, making rare gas lamps an ideal light source for organic molecules [*Butcher et al.*, 1999]. In recent mass spectrometry studies, lamp sources with photon intensities on the order of 10^{13}-10^{14} photons sec^{-1} have been reported [*Hanold et al.*, 2004; *Kuribayashi et al.*, 2005]. In other studies, a rare gas lamp pumped with electrons was used to provide a focused source of VUV photons at the excimer emission lines [*Mühlberger et al.*, 2005a; *Mühlberger et al.*, 2005b]. Most recently, this lamp was used to examine urban aerosol species desorbed from a filter using a combination of thermal pyrolysis and photoionization time-of-flight mass spectrometry [*Streibel et al.*, 2006].

In this Phase II project, we developed a VUV lamp-based photoionization module that can be used together with electron impact (EI) ionization within an Aerodyne Aerosol Mass Spectrometer to provide improved organic speciation. We designed a compact, robust field-deployable VUV module that is compatible with the current AMS, and obtained the first field results with this technique. The complementary information provided by the EI and VUV spectra for both bulk aerosol and size-segregated aerosol is illustrated for a number of pure and mixed organic aerosol particles. Lastly, the results from the VUV module are closely compared to similar experiments conducted using the tunable VUV radiation at the Advanced Light Source in Berkeley, CA. The sensitivities and limits of detection of this method and its potential application for real-time organic aerosol analysis are discussed.

Experimental

1. ToF-AMS

The Aerodyne Aerosol Mass Spectrometer (AMS) has been described in detail elsewhere [*Jayne et al.*, 2000; *Canagaratna et al.*, 2007]. For this study the new, time-of-flight (TOF) version of the AMS referred to as the ToF-AMS was used, where the traditional quadrupole mass spectrometer has been replaced by a compact orthogonal extraction time-of-flight mass spectrometer. The ToF-AMS instrument [*Drewnick et al.*, 2005] and the high-resolution version of the same instrument [*DeCarlo et al.*, 2006] have been described previously; hence, the relevant details are only described here.

As in the case of the quadrupole AMS, aerosol particles are sampled into the ToF-AMS using an aerodynamic lens [*Zhang et al.*, 2002]. The particles exit the lens through a 1 mm i.d. channel skimmer, which skims most of the remaining air and transmits the particle beam into the aerosol-sizing chamber (pressure ~1 x 10^{-5} torr). In this expansion, the particles achieve a terminal velocity depending on their aerodynamic size. The particle beam next encounters a rotating mechanical chopper that "chops" the beam into packets of particles and determines the starting point for each set of particle flight times (chopper cycle 150 Hz, effective duty cycle 2%). After the particles travel through the aerosol sizing chamber they impact on a heated tungsten vaporizer (~600 ºC) and all non-refractory components of the particle vaporize. As the particle plume is created it is immediately ionized via electron impact (EI) with 70 eV electrons emitted by a tungsten filament.

The ions are extracted into the ToF-AMS with a pulse rate of 83.3 kHz, such that when using a mass range of 0 to 300 amu, one mass spectrum takes less than 12 µsec. As this time scale is much less than the time scale of a chopper cycle (150 Hz), many different mass spectra are obtained for different sized particles, and even mass spectra of individual particles are possible. Ions are detected with a chevron-style multi-channel plate (MCP) detector. An important feature of the ToF-AMS is the high-speed (1Gs/s) analog-to-digital converter data card. This board allows for the averaging of raw mass spectra in real time before transfer to a computer. In addition, the card allows for the user to input a noise "threshold" below which all data are discarded. The threshold is set such that it is above the noise level of the data, but below the average signal peak height for a single ion. This allows only ions to be counted as signal, and the measured noise reflects Poisson counting statistics. Because of the relatively low signals in the VUV ionization mode in comparison to the electron impact mode, the "thresholding" feature is critical for improving the signal-to-noise levels and allows for the production of useful signals in minutes.

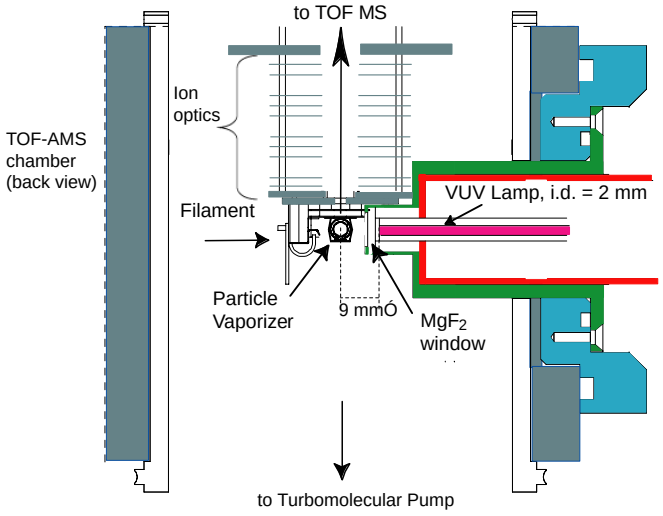

Figure 1. Cross-sectional view of the VUV module and ionization region of the Aerodyne ToF-AMS. The particle beam is aimed into the page.

2. VUV ionization module

A cross section of the modified AMS ionization region is shown in Figure 1. In the typical AMS systems only one filament is run at a time, but two filaments are present to avoid venting the chamber if a filament burns out. To operate in VUV mode, one of the two filaments is removed and replaced with the VUV lamp assembly. The assembly mounts to an existing port on the vacuum chamber, allowing for direct access to the ionization region. The assembly consists of an adapter flange, a stainless steel/window housing, and a module containing the VUV lamp and its associated electronics. The entire assembly weighs about 10 pounds with dimensions of 20 mm x 10 mm x 8 mm. The stainless steel window housing contains a MgF_2 window such that the lamp is operated at atmosphere, but the VUV photons are transmitted through the MgF_2 into the high vacuum of the ionization region. The lamp itself is custom-made by a filling a quartz tube with ~1-3 torr of Krypton gas, a chemical getter (barium azide) and sealing with an MgF_2 window. The VUV light is made through an electrical discharge created through a RF-coil coupling scheme.

Figure 2 shows a typical spectrum of a VUV lamp, with two strong emission lines at 10 and 10.6 eV, (123.6 nm and 118.0 nm respectively). These wavelengths are emitted through as a result of the collisional excitation of Kr atoms and electrons created by the RF-discharge. Each lamp is about 5 cm long with an o.d. of 6 mm and an i.d. of 2 or 3 mm. Thus, the plasma emits from only this small area. The power consumed is about 10-20 watts, where about ~4 watts are internally reflected within the RF power supply. The photon intensity at the exit of the Krypton lamp of the VUV module is estimated to be 5×10^{13} photons sec^{-1}. This estimate, which is

likely only accurate within a factor of 3-4, was obtained by exposing a phototube (Hamamatsu, Shizuoka-ken, Japan) to the lamp and measuring its direct current output after amplification with an analog current amplifier. The average photocathode activity over the entire surface specified by the manufacturer (12 mA / Watt at 121.6 nm) was used in the estimation. Using this value and the active area of the plasma, the total flux at the immediate lamp exit was calculated to be 5 x 10^{14} photons sec^{-1} cm^2. The absolute values shown in Figure 2 have been scaled to reflect this total flux value.

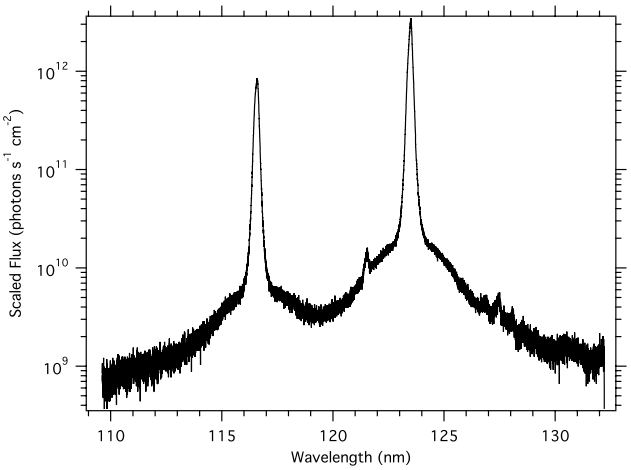

Figure 2. VUV spectrum of a typical Krypton lamp used here, showing the two atomic line emissions at 116.5 nm (10.6 eV) and 123.6 nm (10 eV).

As shown in Figure 1, when the VUV module is connected to the ToF-AMS, the photons enter the ionizer through a 3 mm diameter aperture on its side. The light lost due to this baffling was simulated by placing a 3 mm mask in front of the phototube. From these experiments it was estimated that the VUV beam divergence is about 2 mm per 10 mm (~0.10 steradians), resulting in a total light output at the exit of the lamp of 5 x 10^{14} photons sec^{-1} $steradian^{-1}$. This lamp brightness is similar to those quoted for commercially available VUV lamps of this area. Including both the 1/r2 losses and the baffling effect, the total number of photons reaching the ionizer is estimated to be about 2 x 10^{13} photons sec^{-1}.

3. Aerosol generation

Laboratory aerosols were generated one of two ways. The first method was to dissolve a small amount of sample (usually < 10 mg) in a solvent and use a vibrating critical orifice atomizer to generate a polydisperse sample of pure aerosol with a size mode between 10-1000 nm with a peak at ~100 nm. Using this method, occasionally solvent peaks were observed in the mass spectrum. Pristane was dissolved in dichloromethane, atomized, and dried through a tube filled with activated charcoal. The second method, used generally for oleic acid, was to homogeneously nucleate particles by heating a bath of the pure compound above the necessary supersaturation temperature and subsequently cooling the air. The cigarette smoke aerosol was sampled in the laboratory by burning a cigarette in front of the AMS inlet. This mixture was sampled "in situ" with no pre-concentration.

4. Synchrotron Measurements

To further our understanding of the capability of the VUV photoionization technique within the AMS, a number of experiments were conducted with the AMS at the Chemical Dynamics Beamline of the Advanced Light Source (ALS) at the Lawrence Berkeley National Laboratory. The synchrotron VUV light is generated from an undulator that can be tuned by changing the gap between its magnets to produce VUV light from 7 to 25 eV. The source delivered a highly polarized photon beam of ~10^{16} photons sec^{-1} with a spot size of approximately 1 mm (horizontal) by 0.2 mm vertical directly into the ionization region of the AMS. The AMS was coupled to the light source using a similar set-up to that shown in Figure 1, where the light beam entered the ionization region of the AMS through a vacuum flange on the side of the instrument. The alignment of the beam in the AMS ionizer was carefully tuned by

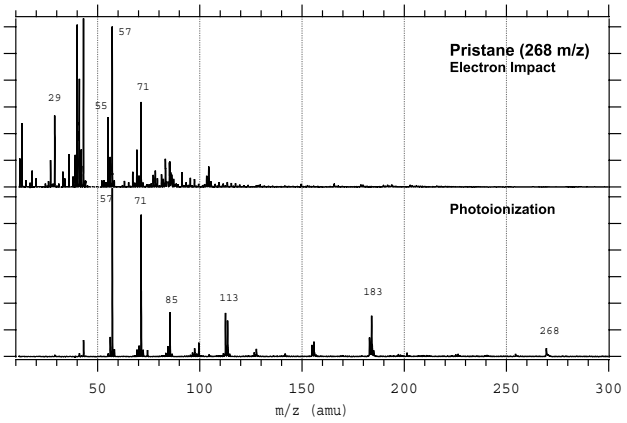

Figure 3. Comparison of ionization techniques for pristane particles.

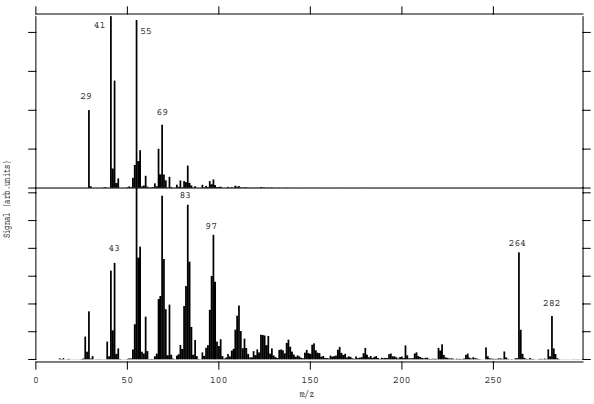

Figure 4. Comparison of EI (top) and PI (bottom) for oleic acid particles at vaporizer temperature of 600 ºC.

both visual alignment using a window and by minute adjustments of the position of the instrument relative to the photon beam.

Results and Discussion for VUV Photoionization (PI) Experiments

1. Comparisons of EI and PI spectra

Figure 3 shows a comparison of electron impact (EI) and photoionization (PI) mass spectra for pristane (IUPAC name = 2,6,10,14-tetramethylpentadecane). Pristane (shown in Figure 3) is a simple, highly branched alkane, which is representative of hydrocarbon-like aerosol material with a high degree of alkyl fragments. The spectrum in Figure 3a highlights the extensive fragmentation that is typically observed in AMS EI spectra for this type of organic species. The EI spectrum is dominated by ions that result from secondary fragmentation of the primary ion fragments (m/z 113, m/z 183, and m/z 253) of pristane [*McLafferty and Turecek*, 1993]. These secondary ions, at m/z=43, 57, and 71, are commonly observed ions for EI spectra of alkanes. The molecular ion at m/z=268 is not visible on a linear scale in the EI spectrum. Although the PI spectrum also contains the ions at m/z=43, 57, and 71, it shows clearly the primary fragments and a prominent peak at the pristine molecular ion on a linear scale. Thus, the PI spectrum provides more specific information about the pristane parent molecule than the EI spectrum.

Figure 4 shows the EI and PI spectra for oleic acid. Since oleic acid has a backbone that consists of a long chain alkane, its EI spectrum has many secondary fragments that are in common with the pristane spectrum. The PI spectrum of oleic acid, on the other hand shows significant differences not only from the oleic acid EI spectrum but also from the pristane PI spectrum. The high mass peaks in the PI spectrum, particularly at the parent ion mass (m/z=282) and the parent ion minus one water molecule (m/z=264 amu) provides a clear signature that can be used more readily than the low m/z EI peaks to identify the oleic acid parent molecule.

Figure 5 compares the EI and PI mass spectra obtained from pure pyrene particles. Since pyrene is a polyaromatic hydrocarbon, its parent ion, which is resistant to fragmentation, is seen as the dominant fragment in both types of spectra. Even for this class of molecules, the PI spectrum is simpler than the corresponding EI spectrum because the PI process does not produce the multiply charged pyrene fragments that are seen in the EI spectrum below m/z 150 amu (*e.g.* the doubly charged pyrene ion at m/z 101). In the EI spectrum the fragments below 150 amu

constitute almost one half of the total ion signal, whereas for the PI spectrum, these fragments are less than 2% of the total ion signal.

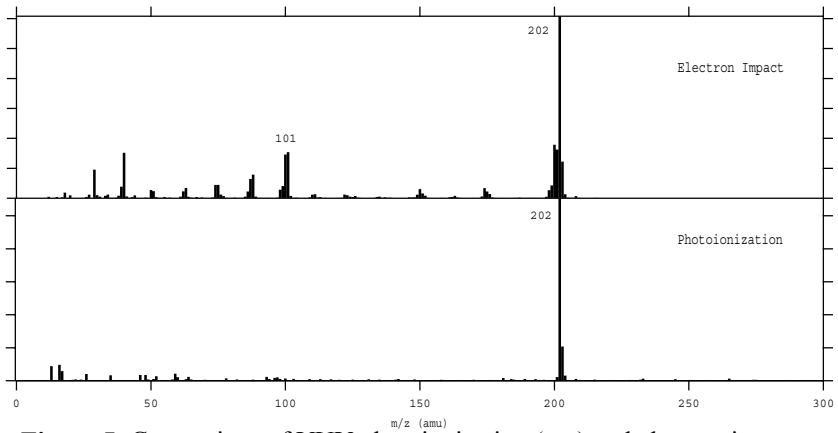

Figure 5. Comparison of VUV photoionization (top) and electron impact ionization (bottom) mass spectra for pyrene (m/z 202).

Figure 6 shows EI and PI spectra for cigarette smoke, which is a rich mixture of unsaturated aliphatic hydrocarbons, carboxylic acids, PAHs, and oxygen and nitrogen heterocyclic aromatic compounds. Overall, the photoionization spectrum differs from the EI spectrum in that it contains many high mass fragments above 100 amu that are visible on the linear scale, including some above 400 amu. Previous studies of cigarette smoke particles reported that although nicotine is a fairly volatile compound, it is an abundant compound found in cigarette smoke particles [*Rogge et al.*, 1994; *Oktem et al.*, 2004]. The molecular mass of nicotine, m/z 162, is a prevalent peak in the PI spectrum, but not in the EI spectrum. The m/z 84 fragment, which dominates the PI spectrum and is present in the EI spectrum, corresponds to another nicotine fragment [*NIST*, 2005]. Although there is signal at almost every peak out to about 400 amu, many of the most dominant peaks are found to be consistent with GC/MS studies on cigarette particles that have identified the individual organic molecules that make up approximately 27% of the measured organic mass[*Rogge et al.*, 1994]. The peaks at m/z values 95 and 146, for example, may correspond to the molecular ions of 3-hydroxypyridine and myosmine which are two heterocyclic nitrogen-containing compounds generally found in large amounts in cigarette smoke particles. The large peak at m/z value 110 could similarly result from the molecular ion of a dominant phenol compound, 1,4-bezenediol in the particles [*Rogge et al.*, 1994]. The hydrocarbon series of high mass peaks at m/z values 380, 394, 408,

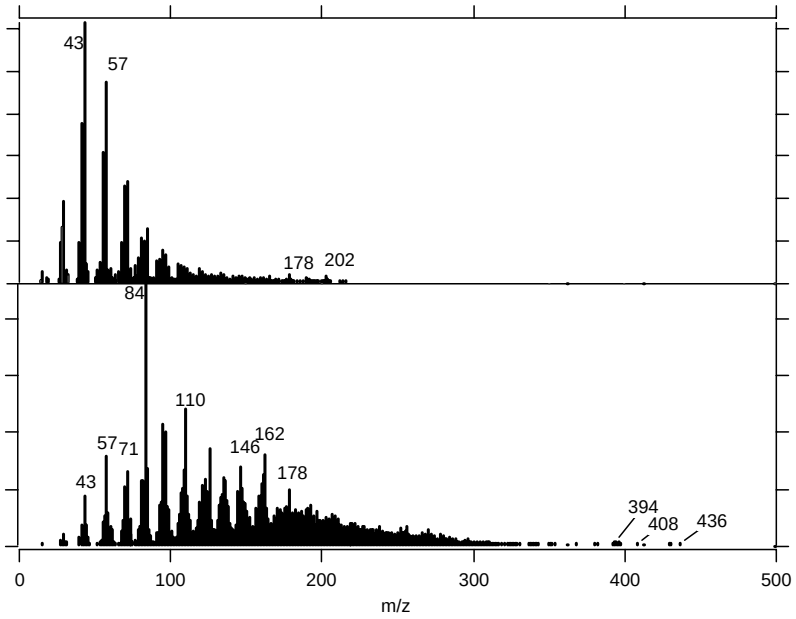

Figure 6. Comparison of electron impact and VUV ionization mass spectra for cigarette smoke.

422, and 436 is consistent with long chain hydrocarbons (C27-C31), which have been found in high loadings in cigarette smoke. The peaks at m/z 178 and m/z 202 are indicative of PAH species anthracene or phenanthrene and pyrene respectively. Since the PAHs are typically resistant to fragmentation, they are observed as parent ions in the EI and PI spectra. As cigarette smoke is such a rich mixture of hundreds of compounds, these peak assignments are tentative at best, but this type of analysis illustrates the way in which PI spectra can enhance the chemical speciation capability of the AMS.

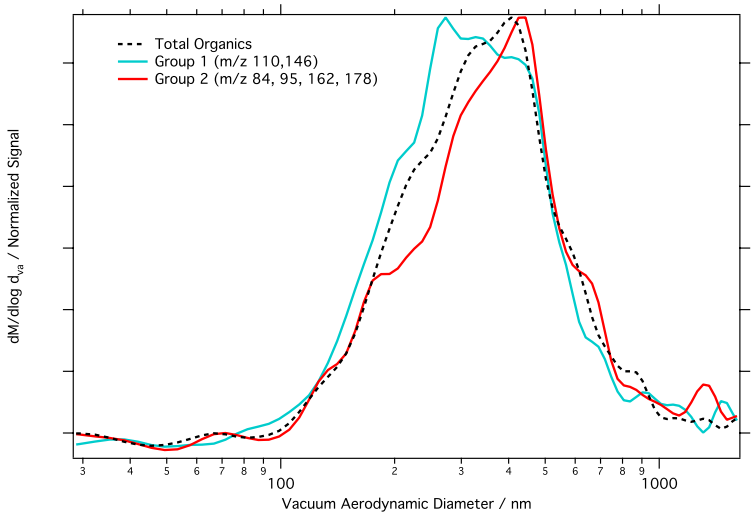

Figure 7. VUV photoionization normalized size distributions from cigarette data for total organics (black line) and the weighted average of selected m/z values (tentative compound assignments from text in parentheses) for Group 1 (blue line): 110 (a benzene diol) and 146 (myosmine), and Group 2: m/z 84 (nicotine fragment), 95 (hydroxypyridine), 162 (nicotine), and 178 (anthracene/phenanthrene) (red line).

Links between aerosol chemical composition and aerosol size can be used to obtain even more detailed information about organic aerosol composition. For example, in previous studies chemically-speciated size distributions have been used in quadrupole-based AMS studies to differentiate between fresh combustion aerosols and aged oxidized organic aerosols [*Alfarra et al.*, 2004; *Canagaratna et al.*, 2007]. The ToF-AMS, when equipped with EI or PI detection, is also capable of providing chemically-speciated particle size distributions. Figure 7 shows the average size dependent distribution for the total organic mass and two groups of individual PI fragments measured while sampling the cigarette smoke particles. Group 1 consists of the m/z values 110, and 146 (likely from a benzene-diol and myosmine, respectively) which peak in signal at around 250 nm. Group 2 consists of nicotine fragments (m/z 162, m/z 84) and other m/z values that are tentatively assigned to hydroxypyridine (m/z 95) and anthracene/phenanthrene (m/z 178). This size distribution peaks near 450 nm. The different size distributions for the two groups of organic ions and fragments clearly indicate that the multiple aerosol modes observed in the average organic distribution have different aerosol organic composition.

Since the ToF-AMS instrument provides a complete EI and PI mass spectrum for every size bin, the size dependence of the cigarette smoke particle composition can be examined in more detail. This is demonstrated in Figure 8 which shows PI mass spectra averaged over the size bins 20-350 nm, 350-600 nm, and 600-1200 nm from Figure 7. The PI mass spectra clearly show differences in the aerosol chemical composition with particle size. The smallest size mode is dominated by the m/z value 110, but the middle and largest size modes are dominated by the nicotine fragment (m/z 84), as in the total mass spectrum (Figure 6). The relative importance of the m/z 178 (possibly PAH) also decreases with size. As illustrated in Figure 6, PI fragments at high m/z contain significant molecular information; hence, they provide more useful and relevant information about the size dependence of aerosol composition than the chemically-speciated size

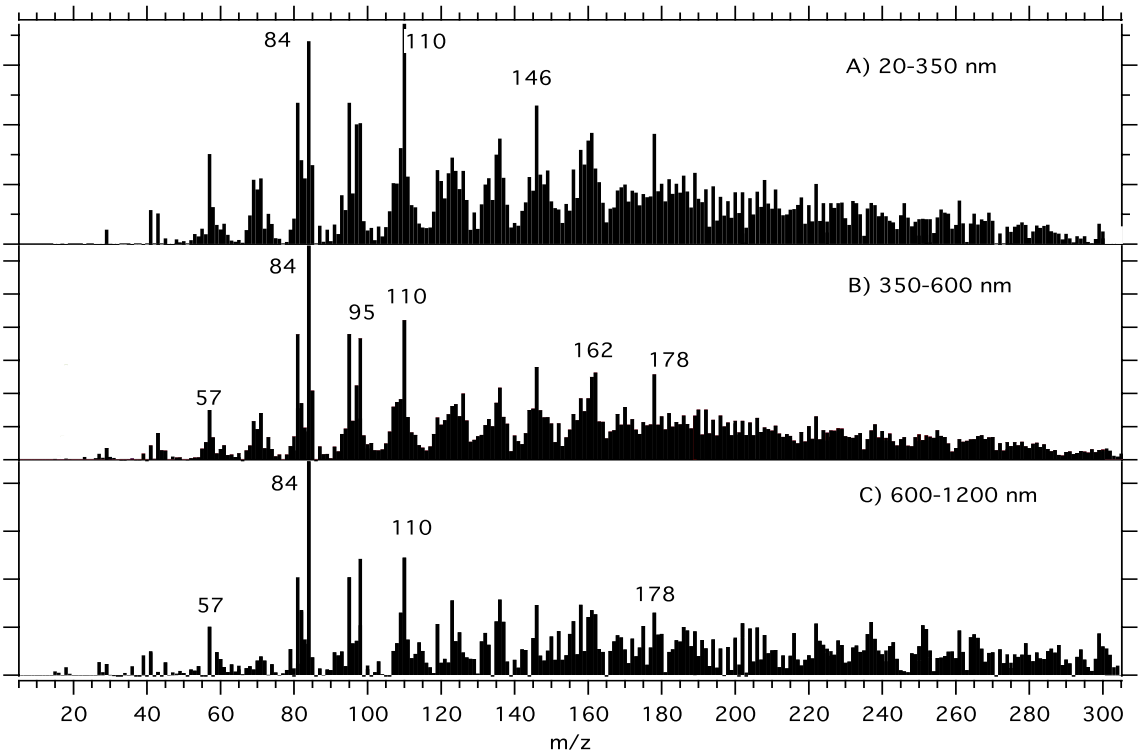

Figure 8. Size-segregated mass spectra for the cigarette smoke particles shown in Figures 6 and 7. Size bins are labeled as A) 20 – 185 nm B) 200-550 nm and C) 600-1000 nm.

distributions measured with EI alone. Thus, the combination of PI with chemically resolved size distributions from the ToF-AMS promises to be a powerful tool for examining size-dependent chemical variations in aerosol composition.

2. Optimizing spectral information available with PI

The exact photoionization spectrum (i.e. degree of fragmentation) from a particular compound depends strongly on both the sample temperature (aerosol vaporization method) and the photoionizing energy used. Both of these factors may contribute excess energy to the ions, resulting in fragmentation of the molecular ion. Previous studies have shown that the degree of fragmentation can be reduced by using lower vaporization temperatures [*Nash et al.*, 2005] or by using a lower photon energy [*Mysak et al.*, 2005; *Nash et al.*, 2005; *Wilson et al.*, 2006]. For example, for the compound oleic acid (shown in Figure 3), other researchers have obtained VUV spectra with very little fragmentation [*Mysak et al.*, 2005]. In order to study the exact fragmentation observed using our system, spectra of oleic acid were taken under a number of varying conditions. Figure 9a shows a spectrum of oleic acid particles taken with the AMS vaporizer temperature at 200 ºC. When compared to Figure 3b (taken at 500 ºC), it is clear that the extent of fragmentation is highly dependent on the thermal energy of the molecular ion. In Figure 9a, relative to the molecular ion (m/z 282) the intensity of the fragment ions (particularly at m/z=84, 98, and 111) has decreased with decreased AMS vaporizer temperature, and the m/z 264 is now the highest peak in the spectrum. The ion fragment at m/z 264 results from the loss of the water ion from the parent ion, likely from thermal degradation and not from a direct ionization process, and is thus a surrogate for the molecular ion of oleic acid. Thus, it may be inferred that a significant amount of fragmentation can be avoided by using oven temperatures just above the boiling point of the compounds of interest.

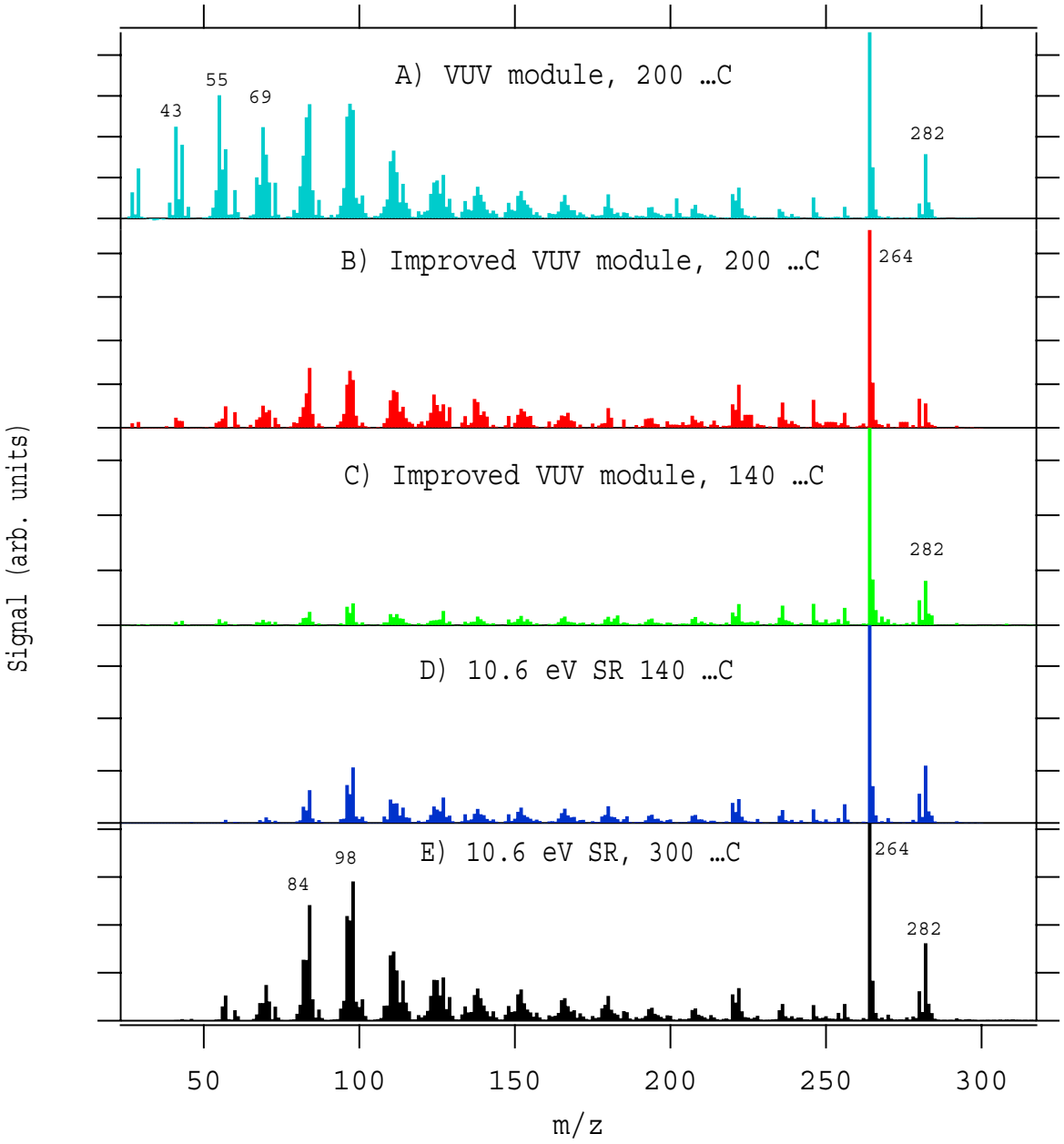

Figure 9. Comparison of VUV photoionization spectra of oleic acid aerosol taken at varying conditions: a) 200 ºC. b) 200 ºC using improved VUV module c) 140 ºC using improved VUV module. d) 140 º C using synchrotron radiation at 10.6 eV e) 300 º C using synchrotron radiation at 10.6 eV

One complication that arises when acquiring PI spectra is unintended electron impact ionization that results from photoelectrons that are formed in the ionization region. Photoelectrons are produced in the ionization region by photons striking metal surfaces of the ionizer. As they are typically formed, these photoelectrons have sufficient energy to ionize the air, water, and oxygen molecules (ionization energies of 12-14 eV) that are present as gas phase molecules in the focused molecular beam but are not photoionized by 10.6 eV VUV. Thus, the presence of these signals is indicative of photoelectron impact occurring in the ionization region. When aerosol signals are small (< 10 ug m^{-3}) these air peaks are sometimes the largest in the

mass spectrum. When photoelectrons are present, electron impact ionization also occurs for vaporized aerosol molecules, causing additional fragmentation of the molecular ion.

The number of photoelectrons can be reduced by minimizing the metal surface area in the system that is exposed to stray and diverging photons from the lamp. We have attempted to do this in our system by bringing the lamp as close as possible to the ionization region of the AMS, thereby minimizing $1/r^2$ divergence of photons from the lamp. The improved design brought the lamp 5 mm closer to the ionizer and improved the number of photoelectrons by an estimated factor of at least 100. This design also improved the photon delivery to the ionization region by a factor of 2, resulting in a corresponding increase in sensitivity. The airbeam and m/z 32 signals were also reduced by greater than a factor of 10. Figures 9a and 9b show a comparison of the photoionization of oleic acid particles at 200 ºC using the previous and modified designs of the VUV module. Although the spectra are very similar above 150 amu, the spectrum from the new design shows a dramatic decrease in the relative intensity of the fragment ions below 100 amu, indicating reduced electron impact. In particular the fragment ions at m/z 43, 55, and 69 seem to be most affected by electron impact and are much reduced with the new design.

In order to quantify the extent to which the electron impact ionization was reduced in the improved VUV module, the oleic acid spectra discussed above were compared with similar experiments carried out at the Advanced Light Source in Berkeley, CA. The synchrotron photon beam was delivered to the AMS in an analogous manner to the VUV lamp module in standard operation. However, because the diameter of the synchrotron photon beam is much smaller than the entrance aperture into the AMS ionizer, the possibility of photoelectron production and electron impact contamination using this source was nearly zero. Figures 9c and 9d show the oleic acid spectrum using the improved VUV module and the synchrotron radiation at 10.6 eV both taken at an AMS vaporizer temperature of 140 ºC. Indeed a visual comparison of these two spectra shows a striking similarity, suggesting that most of the electron impact has been removed in the improved VUV module. Figure 9e shows the oleic acid PI spectrum taken using the synchrotron radiation at 10.6 eV at an AMS vaporizer temperature 300ºC. Note that the fragmentation at 300 ºC (Figure 9e) using the pure photoionization from the SR is notably different from the fragmentation at 200 ºC using the old VUV module (Figure 9a), providing evidence that much of the fragmentation in 9a is due to electron impact ionization and not excess thermal energy. In particular, the fragments at m/z 84 and 98 and are increased from thermal energy, but not those at m/z 43, 55, and 69.

Figure 10 shows the results of synchrotron experiments that mapped the PI spectra of oleic acid as a function of VUV energy and AMS vaporizer temperature. The ratio of the molecular ion sum (m/z 282 + m/z 264) to the total ion signal (designated M^+/Total Ion) is maximized for all temperatures near the ionization energy of 8.7 eV [*Mysak et al.*, 2005]. At this point and the lowest temperatures, more than 75% of the signal is in the parent ion signal. As expected, increased AMS vaporizer temperature causes an increase in fragmentation at all energies above the ionization energy. However, the value of M^+/Total Ion reaches a maximum for all profiles around 100 ºC. Below this temperature there is very little excess thermal energy, however near this temperature the total signal does begin to decrease and vaporization of the oleic acid aerosol is presumably no longer a “flash vaporization” process. Thus, it is important to find an optimum temperature where all of the aerosol is vaporized, but thermal fragmentation is still minimized.

3. Sensitivity and limits of detection

The ionization efficiency in the AMS with the EI or PI process can be expressed as:

(1) $$IE = \sigma \cdot F \cdot \tau \cdot E$$

where σ is the appropriate ionization cross-section of the molecule of interest, F is the ionizing photon or electron flux, τ is the residence time available for ionization, and E is the ion transmission and detection efficiency of the mass spectrometer. Thus, for a given mass spectrometer where τ and E do not vary, the relative IE for electron impact compared with photoionization can be expressed as:

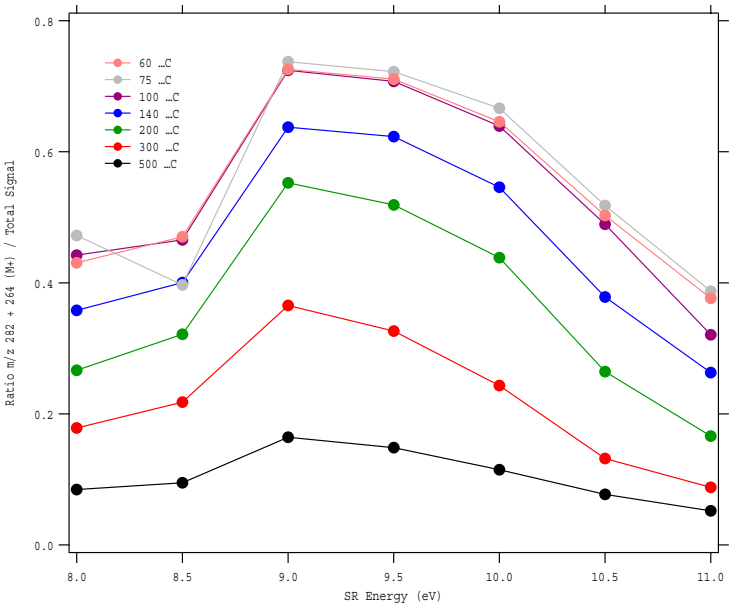

Figure 10. Temperature and VUV photon energy dependence for photoionization of oleic acid using synchrotron radiation.

(2) $$IE_{EI}/IE_{PI} = (\sigma_{EI}/\sigma_{PI}) \cdot (F_{EI}/F_{PI}).$$

In general, for organic molecules the cross-section values for photoionization are 20-70 times less than the cross-section values for electron impact ionization [*Berkowitz*, 2002; *Cool et al.*, 2003; *Jiménez et al.*, 2003]. During EI ionization, the AMS ionizer is usually operated at an emission current of 2.5 mA, which roughly corresponds to an electron output of 1 x 10^{16} electrons sec^{-1}. Since the particle plume is confined by the ionizer and much smaller than the volume of light from the lamp (or electrons from the filament in the case of EI), the ionizing volume for both processes is assumed to be the same, and the value of F_{EI}/F_{PI} is approximately equal to the ratio of electron output to photon output for the two processes (units of photons sec^{-1} or electrons sec^{-1}). As discussed above in the Experimental section, the VUV lamp yields an output of 2 x 10^{13} photons sec^{-1} at the ionizer, such that the value of F_{EI}/F_{PI} is 500. Thus taken together, according to equation 1.2 above, the IE_{EI}/IE_{PI} is estimated to be 1 x 10^{4}.

For the both the quadrupole and the ToF-AMS instruments the IE_{EI} is routinely measured as a metric of the instrument sensitivity and stability[*Jiménez et al.*, 2003]. The calibration procedure involves the use of size-selected particles of known concentration. The IE is defined as the ratio of the average measured number of ions per particle to the known number of molecules per particle. The IE_{PI} has been measured by an analogous procedure for oleic acid. As summarized in Table 1, a typical measured value for IE_{EI} (for 70 eV electron impact) in a ToF-AMS for oleic acid is 1 x 10^{-6} and the measured IE_{PI} of oleic acid is 2 x 10^{-10}. The ratio of these measured values, 5000, is within a reasonable factor of 2 of the estimated value from equation 1.2.

The detection limit in EI mode for organic species in a 1-minute average spectrum is approximately 1 ng m^{-3}. Because the thresholding feature of the Acqiris data acquisition card

can be used to discriminate against electronic noise, the instrument noise can be reduced to simply the dark counts of the MCP. For a new set of MCPs this value can be as low as 1 count per minute, although values of 2-5 counts per second are more typical. For the experiments here, the RMS noise calculated for the difference signal with no particles (filter measurement) is typically around 0.002 bits per extraction, which corresponds to 3 μg m^{-3} for a 1-minute average. Thus, the 3σ limit of detection for oleic acid is calculated to be about 12 μg m^{-3} for a 1-minute average, based on the measured ionization efficiency for this molecule shown in Table 1. Limits of detection for many other organic molecules will generally be in the same range, depending on the specific photoionization cross section of the molecule. For some ions (e.g. m/z 43), there is a significant gas-phase background that increases the limit of detection for aerosol signals. Furthermore, at very high mass loadings, ions scattering in the ion flight region also will affect the limits of detection.It is clear from Table 1, that the sensitivity of PI relative to EI can be improved by increasing the photon flux of the VUV lamp. The photon output of the lamp used in these studies is likely within a factor of 10 of its theoretical maximum for an unfocused beam. We believe that the plasma is near saturation for two reasons: first, when the input power is increased, the photon flux begins to fall off. Moreover, other commercially available lamps have similar outputs. Resonance, Ltd, in Ontario, Canada, produces lamps with an output of 3 x 10^{15} photons $steradian^{-1}$ sec^{-1} for a 12 mm diameter lamp. The effective area of this lamp is 16 times larger than the 3 mm lamp used for the measurements shown in this manuscript, and therefore actually has a very similar output per area or flux as the lamp used here. Therefore, this lamp would not increase the sensitivity of the VUV module.

Table 1. Sensitivity for EI and PI

	EI ionization	Photoionization (PI)	EI/PI
Flux, part cm^{-2} sec^{-1}	1 x 10^{16} /area	2 x 10^{13} /area	5 x 10^{2}
σ, cm^2 $molec^{-1}$	6 x 10^{-16}	3 x 10^{-17}	20
Measured IE	1 x 10^{-6}	2 x 10^{-10}	5x 10^{3}
Predicted IE_{EI}/IE_{PI}			1 x 10^{4}

Other researchers have used methods to improve photon fluxes of traditional lamp supplies that do not use a laser. Notably, Mühlberger et al. [2005a; 2005b] have developed the Electron-Beam-Pumped Excimer VUV lamp, whereby a Kr or Ar source is irradiated with electrons from an electron gun to create rare gas excimers using single photon ionization. Reported photon intensities are presently about 1.5 x 10^{13} photons s^{-1}, but are expected to increase by a factor of ten in the near future [*Mühlberger et al.*, 2005b]. If indeed such lamps eventually create more photons than the rare gas lamps of a similar size, than using such a lamp with the AMS may be a promising alternative for increasing the sensitivity of the technique.

Another approach is to use the photons from the VUV lamp not for direct ionization but for the ejection of photoelectrons from a photoemissive surface that is coupled into the AMS. The photoelectrons produced by this method, known as PERCI (Photoelectron Resonance Capture Ionization Mass Spectrometry) [*LaFranchi et al.*, 2004] are finely tuned to a low energy

(<0.1 eV), by the addition of an extra electrode near the photoemissive surface. These low energy photoelectrons attach to analyte molecules resulting in little or no fragmentation. This technique could be a feasible alternative to photoionization.

5. Conclusions for VUV Photoionization

This report presents results obtained from a field-deployable VUV lamp module that can be interfaced to the Aerodyne Aerosol Mass Spectrometer to provide PI spectra of aerosol chemical species in real time *[Northway et al.,* 2007*]*. The results presented here indicate that photoionization using rare gas lamps is a promising ionization technique for improving the molecular information provided by AMS mass spectra. Although the high temperature of the AMS vaporizer induces some thermal fragmentation, the PI spectra are less complicated than EI spectra due to decreased fragmentation. The PI spectra obtained from the VUV lamp are similar to those obtained with VUV radiation from a synchrotron source. Comparisons of EI and PI spectra of pure organic particles show that the presence of parent peaks and characteristic fragments at masses greater than 100 amu in the PI spectra provide clear signatures for chemical identification. Even in more complex organic mixtures such as cigarette smoke particles, the PI spectra provide more information about the molecular composition of the aerosol than EI spectra. Speciated size distributions measured with the PI detection technique offer an additional means of increasing the chemical information that can be obtained by the AMS for complex mixtures of aerosol particles.

The reported PI detection limits of 1-5 $\mu g\ m^{-3}$ are sufficient for laboratory work, source sampling, and detection of atmospheric aerosol in polluted urban atmospheres at fixed sites. The PI spectra presented here, however, are limited by photon fluxes in comparison to electron fluxes in electron impact ionization, and span only 3-4 orders of magnitude in signal in comparison to the 7 orders of magnitude spanned by the current AMS in standard electron impact mode. With several ongoing advances in excimer rare gas lamp technology there is a significant potential of improving the sensitivity of the photoionization technique by a factor of 50-100, which would be similar to the existing quadrupole AMS instruments.

A key feature of the VUV lamp module design is its ability to alternate between PI and EI detection on the timescale of minutes. This feature allows for the exploitation of the advantages of both detection techniques. While PI offers spectral simplicity, alternation of PI with the EI allows for increased sensitivity to organic aerosol mass and maintains the AMS sensitivity to inorganic species like SO_4 and NO_3 which are not effectively ionized by 10.6 eV PI. The ability to alternate PI detection with EI is also important because electron impact ionization efficiency has an empirical dependence on chemical composition and molecular weight that can be readily used to quantify speciated mass.

Soft Ionization with Dissociative Electron Attachment

The time-of-flight mass spectrometers (manufactured by Tofwerk AG, Thun, Switzerland) used on the ToF-AMS are available in a bipolar configuration, allowing for the detection of negative ions. This opens up the possibility of ionization by dissociative electron attachment, in which the electrons from the EI source are captured by the organics, and the resulting anions are detected in the mass spectrometer. To maximize electron attachment (minimize ion fragmentation), the energy of the electron source is reduced (to <30 eV). This technique is particularly powerful for the detection of organic acids, which are deprotonated upon electron impact:

(3) $$RCOOH + e^- \rightarrow RCOO^- + H$$

This ionization technique is of particular interest because organic acids are known to be a major component of SOA. Other SOA components include oxidized organics such as esters and nitrates, which are also expected to be efficiently ionized by this technique. Shown in Figure 11 is a dissociative electron attachment mass spectrum of SOA from trimethylbenzene (TMB) photooxidation, generated in the environmental chamber at the Paul Scherrer Institute (Zurich, Switzerland). A large number of individual organic acids can be seen, some of which have been identified previously using offline mass spectrometric techniques (derivatization/GC-MS, electrospray ionization, atmospheric pressure chemical ionization, etc.). Molecular identification is straightforward, as fragmentation of the organic acids is minimal. The dominant m/z peak from each is the deprotonated molecular ion. Dissociative electron attachment ionization is now a routine approach for all AMS systems configured for bipolar, negative ion detection.

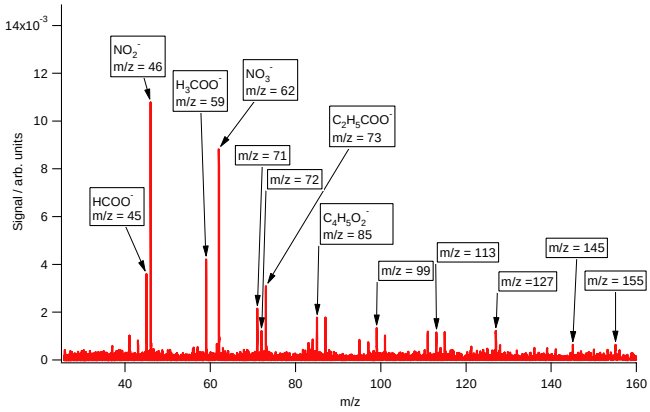

Figure 11. AMS mass spectrum of SOA from TMB photooxidation, using dissociative electron attachment ionization.

Soft Ionization with Low-energy Electron Impact.

Ionization by low-energy electrons from the EI source will also form positive ions.

(4) $$R + e^- \rightarrow R^+ + 2e^-$$

This is essentially the same ionization scheme which is operative in standard EI, only the much lower energies of the electrons (~10-12 eV) will lead to far lower fragmentation of the molecular ion, greatly facilitating chemical characterization of the organic species present in the aerosol. This ionization scheme is available as a routine measurement on all AMS systems. This technique was used in Mexico City as part of the DoE-funded MILAGRO/MAX MEX campaign, and results are shown in Figure 12. In the left panel is a low-energy EI mass spectrum of ambient aerosol measured in Mexico City. While there is clearly some degree of fragmentation of organic species, it is far less than is seen in standard (70 eV) EI, and individual higher-mass peaks begin to emerge. From the time traces of these peaks (right panel of Figure 12), it is clear the signals from some species change dramatically, even when total organic mass stays relatively constant. This strongly suggests these peaks correspond to individual molecular markers, possibly for SOA formation. Detection of individual markers in real time represents a significant advance over off-line techniques, which involve collecting samples over the course of several hours and suffer from very low time resolution. This approach has the advantage of being directly applicable to all AMS systems and the disadvantage that the relative wide spread

in electron energies leads to the significant fragmentation apparent in the signals for m/z < 100 in Fig 12.

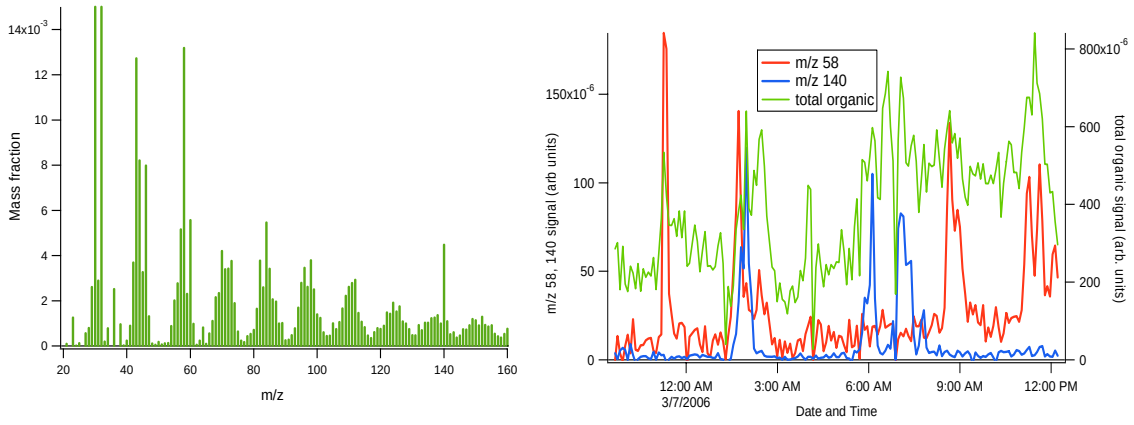

Figure 12. Results from AMS measurements made near downtown Mexico City in 2006 (as part of the MILAGRO/MAX MEX campaign), using low energy electron impact ionization. Left panel: average mass spectrum from a 14-hour period. Right panel: time trace of total organic signal (in green) and two individual "marker" ions (m/z 58 and m/z 140).

Soft Ionization with Lithium Ion Attachment.

The fourth soft ionization approach developed for use in the AMS is a chemical ionization technique, using lithium ions (Li^+) as the ionizing reagent:

(5) $$R + Li^+ + M \rightarrow [R\text{-}Li]^+ + M$$

This is an ion attachment process requiring a third body (M) to remove excess energy from the newly formed ion adduct. We have demonstrated that, despite the low pressures in the AMS ionization region, this is still an efficient soft ionization technique for the measurement of a range of organic species. Alkanes, sugars, fatty acids, and esters, as well as more complex mixtures such as secondary organic aerosol, diesel particles, biomass burning particles, and aged organics, have all been detected in the AMS using this ionization scheme. Fragmentation is minimal, with the dominant ion always being of mass M+6 (the molecular weight of the organic plus the mass of the ^6Li from the ion source), indicating that this technique is exceptionally soft and well-suited for molecular identification. As an example, the AMS spectrum of levoglucosan ($C_6H_{10}O_5$) is shown in Figure 13.

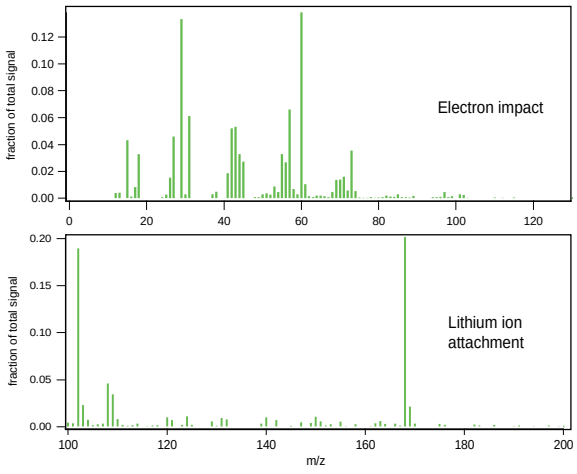

Figure 13. Comparison of electron impact ionization (EI) and Li+ attachment mass spectra for levoglucosan particles. In the lithium attachment spectrum, the only major ions are m/z 168 (M+6) and one fragment at m/z 102. Note the difference in m/z ranges in the two plots: in EI, ion signals above m/z 100 are insignificant; in Li+ ion attachment, ions below m/z 100 are omitted due to "ion blanking" (see below).

One of the primary advantages of the AMS (in its standard EI configuration) is that it is quantitative: total ion signal is proportional to aerosol mass concentrations, making measurements of particulate loading straightforward. For soft ionization techniques such as Li^+ ion attachment to be useful in the real-time measurement of molecular markers, it is important that the measured signal from these techniques be quantitative as well. Shown in Figure 14 (left panel) are results from calibrations of Li^+ ion attachment for levoglucosan, a major aerosol marker for wood-burning. Signal (from m/z 168 or from the major fragment, m/z 102) is proportional to levoglucosan concentration, indicating the quantitative nature of this ionization technique. Additionally, an AMS with the Li^+-ion source was used to measure biomass burning

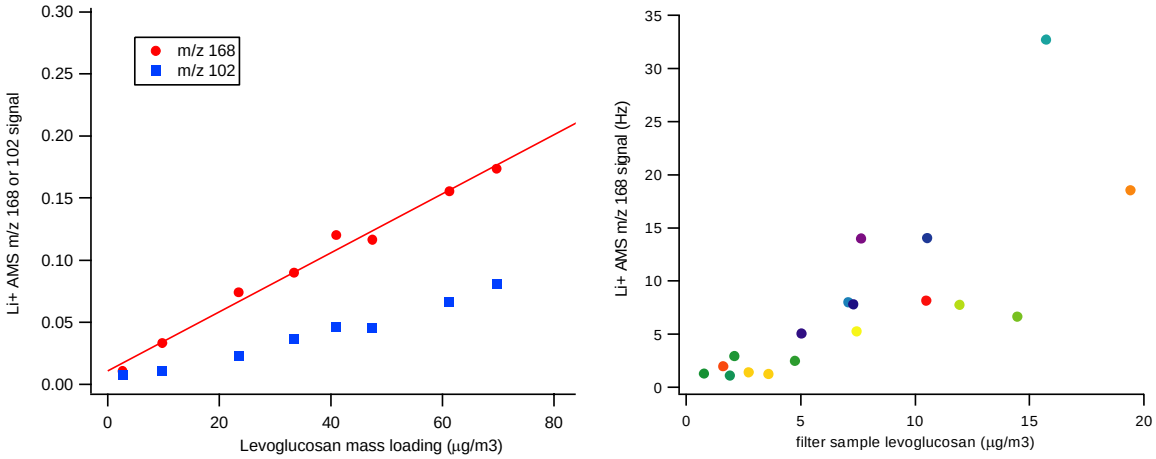

Figure 14. AMS measurements of levoglucosan (a wood burning tracer) using lithium attachment ionization. Left panel: calibration curves, showing the signals of the two major ions in the levoglucosan mass spectrum (the M+6 ion and the m/z 102 fragment) vs. levoglucosan mass loading. Right panel: measurements of levoglucosan in biomass burning aerosol (during the FLAME study), comparing results from the AMS with Li-ion attachment and with those from an offline technique. Each point corresponds to a single biomass burn.

aerosol during the FLAME (Fire Lab At Missoula Experiment) study, and levoglucosan concentrations within the particles were measured. In the right panel of Figure 14, a comparison of our Li^+-attachment AMS results with measurements by an offline technique (collection by Hi-Vol sampling and analysis using high-performance anion exchange chromatography) are shown.

Aerosol mass spectrometry with lithium-ion attachment ionization was also successfully deployed at the T0 site in Mexico City as part of the 2006 MILAGRO campaign. In the left panel of Figure 15 is an average mass spectrum taken over a 36-hour period; the spectrum is relatively sparse, dominated by a few high-mass peaks, indicating the selectivity of this technique to certain classes of organics. Some of these peaks (such as m/z 213) were also seen in the FLAME study, indicating a likely biomass burning origin of the aerosol; others are expected to be tracers of secondary organic aerosol. Time traces of some of these peaks are shown in the right panel of Figure 15. Concentrations of the individual species vary dramatically on the time scale of ~1 hour, underscoring the utility of this technique in providing real-time measurements of molecular markers in the aerosol, which are expected to be of use in source apportionment for urban aerosols.

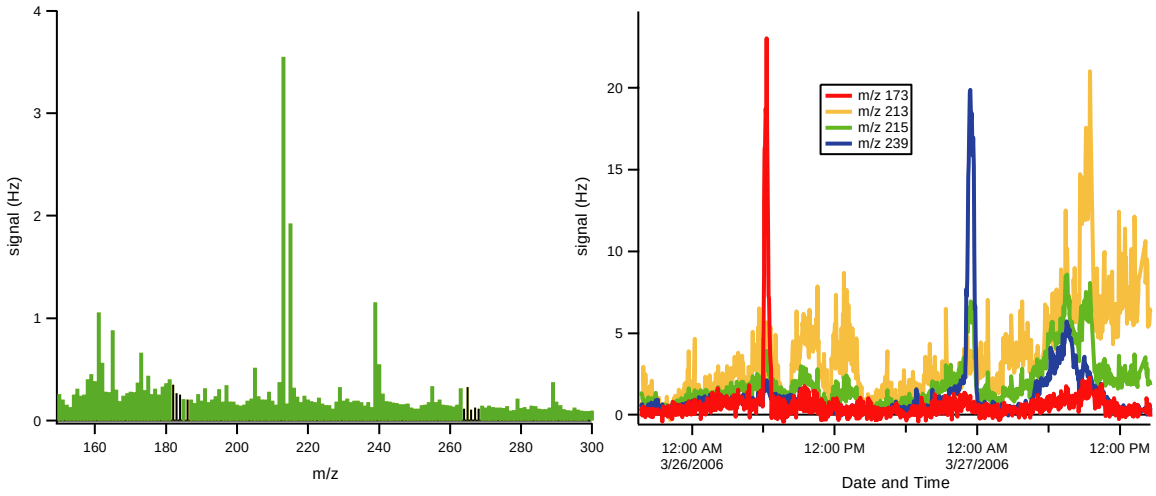

Figure 15. Results from AMS measurements during the 2006 MILAGRO campaign using lithium-ion attachment ionization. Left panel: average mass spectrum for a 36 hour period. Right panel: time traces of individual ions.

Conclusion

During this DOE SBIR Phase II project, we have successfully developed several soft ionization techniques, i.e., ionization schemes which involve less fragmentation of the ions, for use with the ToF-AMS. Vacuum ultraviolet single photon ionization was demonstrated in the laboratory and deployed in field campaigns [*Northway et al.*, 2007]. This demonstration has led to collaboration with a German group [*Mühlberger et al.*, 2005b] to continue VUV lamp development undertaken by the University of Colorado during the SBIR. Dissociative electron attachment with lower energy electrons (<30 eV) was demonstrated in the measurement of particulate organics in chamber experiments in Switzerland, and is now a routine approach with AMS systems configured for bipolar, negative ion detection. This technique is particularly powerful for detection of acidic and other highly oxygenated SOA chemical functionality. Low energy electron ionization (10-12 eV) is also a softer ionization approach routinely available to AMS users. Finally, Lithium ion (Li^+) attachment has been shown to be sensitive to more alkyl-like chemical functionality in SOA. Results from Mexico City are particularly exciting in observing changes in SOA molecular composition under different photochemical/meteorological conditions. More recent results detecting biomass burns at the Montana fire lab have demonstrated quantitative and selective detection of levoglucosan.

These soft ionization techniques provide the ToF-AMS with better capability for identifying organic species in ambient atmospheric aerosol particles. This, in turn, will allow more detailed study of the sources, transformations and fate of organic-containing aerosol.

Publications Resulting from this Project (attached at end of report)

Northway, M.J., J.T. Jayne, D.W. Toohey, M.R. Canagaratna, A. Trimborn, K.-I. Akiyama, A. Shimono, J.L. Jiménez, P.F. DeCarlo, K.R. Wilson, and D.R. Worsnop, Demonstration of a VUV lamp photoionization source for improved organic speciation in an aerosol mass spectrometer, *Aerosol Science & Technology*, *41*, 829-839, 2007.

Conference Papers Resulting from this Project (abstracts attached at end of report)

Onasch, T. B., A. Trimborn, J. Kroll, D. Worsnop, I. Ulbrich, J. A. Huffman, J. Jimenez, S. Kreidenweis, W. M. Hao, The chemical and physical characteristics of biomass burning particulate emissions studied at the Fire Science Laboratory, 2007 AAAR Annual Conference, Reno, NV.

Trimborn, A., T. Onasch, M. Canagaratna, J. Kroll, D. Trimborn, M. Cubison, J. Jimenez, J. Jayne, D. Worsnop, Ionization methods used in the Aerodyne AMS, 2007 FACSS Conference, Memphis, TN.

Trimborn, A., J. Jayne, M. Northway, T. Onasch, K. Akiama, D. Worsnop, First Field Deployments of an Aerodyne AMS Using Lithium Ion Attachment Ionization to Characterize Ambient Organic Aerosol Particles, 2006 AGU Fall Meeting, San Francisco, CA.

Trimborn, A., J. Jayne, M. Northway, T. Onasch, K. Akiama, D. Worsnop, Lithium ion attachment as a soft ionization approach for detection of organic species in the Aerodyne AMS, 2006 ASMS Conference, Seattle, WA.

References

Alfarra, M.R., H. Coe, J.D. Allan, K.N. Bower, H. Boudries, M.R. Canagaratna, J.L. Jiménez, J.T. Jayne, A. Garforth, S.M. Li, and D.R. Worsnop, Characterization of Urban and Regional Organic Aerosols in the Lower Fraser Valley using two Aerodyne Aerosol Mass Spectrometers, *Atmos. Env.*, *38*, 5745-5758, 2004.

Alfarra, M.R., D. Paulsen, M. Gysel, A.A. Garforth, J. Dommen, A.S.H. Prévôt, D.R. Worsnop, U. Baltensperger, and H. Coe, A mass spectrometric study of secondary organic aerosols formed from the photooxidation of anthropogenic and biogenic precursors in a reaction chamber, *Atmospheric Chemistry and Physics Discussions*, *6*, 7747-7789, 2006.

Bahreini, R., M.D. Keywood, N.L. Ng, V. Varutbangkul, S. Gao, R.C. Flagan, J.H. Seinfeld, D.R. Worsnop, and J.L. Jimenez, Measurements of Secondary Organic Aerosol (SOA) from oxidation of cycloalkenes, terpenes, and m-xylene using an Aerodyne Aerosol Mass Spectrometer, *Env. Sci. and Tech.*, *39*, 5674-5688, 2005.

Berkowitz, J., *Atomic and Molecular Photoabsorption: Absolute Total Cross Sections*, Academic Press, 2002.

Butcher, D.J., D.E. Goeringer, and G.B. Hurst, Real-time determination of aromatics in automobile exhaust by single-photon ionization ion trap mass spectrometry, *Anal. Chem.*, *71* (2), 489-496, 1999.

Canagaratna, M.R., J.T. Jayne, J.L. Jiménez, J.D. Allan, M.R. Alfarra, Q. Zhang, T.B. Onasch, F. Drewnick, H. Coe, A. Middlebrook, A. Delia, L.R. Williams, A.M. Trimborn, M.J. Northway, P.F. DeCarlo, C.E. Kolb, P. Davidovits, and D.R. Worsnop, Chemical and Microphysical Characterization of Ambient Aerosols with the Aerodyne Aerosol Mass Spectrometer, *Mass Spectrometry Reviews*, *26*, 185-222, 2007.

Cao, L., F. Muhlberger, T. Adam, T. Streibel, H.Z. Wang, A. Kettrup, and R. Zimmermann, Resonance-enhanced multliphoton ionization and VUV-single photon ionization as soft and selective laser ionization methods for on-line time-of-flight mass spectrometry: Investigation of the pyrolysis of typical organic contaminants in the steel recycling process, *Anal. Chem.*, *75* (21), 5639-5645, 2003.

Cool, T.A., K. Nakajima, T.A. Mostefaoui, F. Qi, A. McIlroy, P.R. Westmoreland, M.E. Law, L. Poisson, D.S. Peterka, and M. Ahmed, Selective detection of isomers with photoionization mass spectrometry for studies of hydrocarbon flame chemistry, *J. Chem. Phys.*, *119*, 8356, 2003.

DeCarlo, P.F., J.R. Kimmel, A. Trimborn, M.J. Northway, J.T. Jayne, A.C. Aiken, M. Gonin, K. Fuhrer, T. Horvath, K. Docherty, D.R. Worsnop, and J.L. Jiménez, A Field-Deployable High-Resolution Time-of-Flight Aerosol Mass Spectrometer, *Analytical Chemistry*, *78*, 8281-8289, 2006.

Dockery, D.W., C.A. Pope, X.P. Xu, J.D. Spengler, J.H. Ware, M.E. Fay, B.G. Ferris, and F.E. Speizer, An Association between Air-Pollution and Mortality in 6 United States Cities, *New England Journal of Medicine*, *329* (24), 1753-1759, 1993.

Drewnick, F., S.S. Hings, P.F. DeCarlo, J.T. Jayne, M. Gonin, K. Fuhrer, S. Weimer, J.L. Jiménez, K.L. Demerjian, S. Borrmann, and D.R. Worsnop, A new Time-of-Flight Aerosol Mass Spectrometer (ToF-AMS) – Instrument Description and First Field Deployment, *Aerosol Sci. Tech.*, *39*, 637–658, 2005.

Hanold, K.A., S.M. Fischer, P.H. Cormia, C.E. Miller, and J.A. Syage, Atmospheric pressure photoionization. 1. General properties for LC/MS, *Anal. Chem.*, *76*, 2842-2851, 2004.

Heger, H.J., R. Zimmerman, R. Dorfner, M. Beckmann, H. Griebel, A. Kettrup, and U. Boesl, On-line Emission Analysis of Polycyclic Aromatic Hydrocarbons down to ppt Concentration Levels in the Flue Gas of an Incineration Pilot Plant with a Mobile Resonance Enhanced Multiphoton Ionization Time-of-Flight Mass Spectrometer, *Anal. Chem.*, *71* (1), 46-57, 1999.

IPCC, *Climate Change 2007: The Physical Scientific Basis*, Cambridge University Press, Cambridge, England, 2007.

Jayne, J.T., D.C. Leard, X. Zhang, P. Davidovits, K.A. Smith, C.E. Kolb, and D.R. Worsnop, Development of an Aerosol Mass Spectrometer for Size and Composition Analysis of Submicron Particles, *Aerosol Sci. Technol.*, *33*, 49-70, 2000.

Jiménez, J.L., J.T. Jayne, Q. Shi, C.E. Kolb, D.R. Worsnop, I. Yourshaw, J.H. Seinfeld, R.C. Flagan, X. Zhang, K.A. Smith, J. Morris, and P. Davidovits, Ambient aerosol sampling using the Aerodyne Aerosol Mass Spectrometer, *J. Geophys Res.*, *108* (D7), 8425 doi:10.1029/2001JD001213, 2003.

Kalberer, M., D. Paulsen, M. Sax, M. Steinbacher, J. Dommen, A.S.H. Prevot, R. Fisseha, E. Weingartne, V. Frankevich, R. Zenobi, and U. Baltensperger, Identification of polymers as major components of atmospheric organic aerosols, *Science*, *303*, 1659-1662, 2004.

Kuribayashi, S., H. Yamakoshi, M. Danno, S. Sakai, S. Tsuruga, H. Futami, and S. Morii, VUV Single-photon ionization ion trap time-of-flight mass spectrometer for on-line, real-time monitoring of chlorinated organic compounds in waste incineration flue gas, *Anal. Chem.*, *77*, 1007-1012, 2005.

LaFranchi, B.W., J. Zahardis, and G.A. Petrucci, Photoelectron resonance capture ionization mass spectrometry: a soft ionization source for mass spectrometry of particle-phase organic compounds, *Rapid Comm. Mass Spec.*, *18* (21), 2517-2521, 2004.

McLafferty, F.W., and F. Turecek, *Interpretation of mass spectra*, 6-7 pp., University Science Books, Mill Valley, CA, 1993.

Mühlberger, F., T. Streibel, J. Wieser, A. Ulrich, and R. Zimmermann, Single-Photon Ionization Time-of-Flight Mass Spectrometry with a Pulsed Electron Beam Pumped Excimer VUV

Lamp for On-Line Gas Analysis: Setup and First Results on Cigarette Smoke and Human Breath, *Anal. Chem*, *77* (22), 7408-7414, 2005a.

Mühlberger, F., J. Wieser, A. Morozov, A. Ulrich, and R. Zimmermann, Single-Photon Ionization Quadrupole Mass Spectrometry with an Electron Beam Pumped Excimer Light Source, *Anal. Chem.*, *77*, 2218-2226, 2005b.

Mühlberger, F., J. Wieser, A. Ulrich, and R. Zimmermann, Single Photon Ionization (SPI) via Incoherent VUV-Excimer Light: Robust and Compact Time-of-Flight Mass Spectrometer for On-Line, Real-Time Process Gas Analysis, *Anal. Chem*, *74* (15), 3790-3801, 2002.

Mühlberger, F., R. Zimmermann, and A. Kettrup, A mobile mass spectrometer for comprehensive on-line analysis of trace and bulk components of complex gas mixtures: parallel application of the laser-based ionization methods VUV single-photon ionization, resonant multiphoton ionization, and laser-induced electron impact ionization, *Anal. Chem.*, *73*, 3590-3604, 2001.

Murphy, D.M., Something in the Air, *Science*, *307*, 1888-1890, 2005.

Murphy, D.M., D.S. Thomson, and T.M.J. Mahoney, In situ measurements of organics , meteoritic material, mercury, and other elements in aerosols at 5 to 19 kilometers, *Science*, *282*, 1664-1669, 1998.

Mysak, E.R., K.R. Wilson, M. Jimenez-Cruz, M. Ahmed, and T. Baer, Synchrotron radiation based aerosol time-of-flight mass spectrometry for organic constituents, *Anal. Chem*, *77* (18), 5953-5960, 2005.

Nash, D.G., X.F. Liu, E.R. Mysak, and T. Baer, Aerosol particle mass spectrometry with low photon energy laser ionization, *Int. J. Mass Spectrom.*, *241*, 89-97, 2005.

NIST, NIST Chemistry WebBook, NIST Standard Reference Database Number 69, National Institute of Standards and Technology, 2005.

Noble, C.A., and K.A. Prather, Real-time single particle mass spectrometry: A historical review of a quarter century of the chemical analysis of aerosols, *Mass Spectrom. Rev.*, *19*, 248, 2000.

Northway, M.J., J.T. Jayne, D.W. Toohey, M.R. Canagaratna, A. Trimborn, K.-I. Akiyama, A. Shimono, J.L. Jiménez, P.F. DeCarlo, K.R. Wilson, and D.R. Worsnop, Demonstration of a VUV lamp photoionization source for improved organic speciation in an aerosol mass spectrometer, *Aerosol Science & Technology*, *41*, 829-839, 2007.

Oktem, B., M.P. Tolocka, and M.V. Johnston, On-Line Analysis of Organic Components in Fine and Ultrafine Particles by Photoionization Aerosol Mass Spectrometry, *Anal. Chem.*, *76* (2), 253-261, 2004.

Robinson, A.L., N.M. Donahue, M.K. Shrivastava, E.A. Weitkamp, A.M. Sage, A.P. Grieshop, T.E. Lane, J.R. Pierce, and S.N. Pandis, Rethinking Organic Aerosols: Semivolatile Emissions and Photochemical Aging, *Science*, *315*, 1259-1262, 2007.

Rogge, W.F., L.M. Hildemann, M.A. Mazurek, G.R. Cass, and B.R.T. Simoneit, Sources of Fine Organic Aerosol. 6. Cigaret Smoke in the Urban Atmosphere, *Env. Sci. Tech.*, *28* (7), 1375-1388, 1994.

Streibel, T., J. Weh, S. Mitschke, and R. Zimmermann, Thermal Desorption/Pyrolysis Coupled with Photoionization Time-of-Flight Mass Spectrometry for the Analysis of Molecular Organic Compounds and Oligomeric and Polymeric Fractions in Urban Particulate Matter, *Anal. Chem*, *78* (15), 5354-5361, 2006.

Sykes, D.C., I. E. Woods, G.D. Smith, T. Baer, and R.E. Miller, Thermal vaporization-vacuum ultraviolet laser ionization time-of-flight mass spectrometry of single aerosol particles, *Anal. Chem.*, *74* (9), 2048-2052, 2002.

Volkamer, R., J.L. Jiménez, F. San Martini, K. Dzepina, Q. Zhang, D. Salcedo, L.T. Molina, D.R. Worsnop, and M.J. Molina, Secondary Organic Aerosol Formation from Anthropogenic Air Pollution: Rapid and Higher than Expected, *Geophys. Res. Lett.*, *33*, L17811, doi:10.1029/2006GL026899, 2006.

Watson, J.G., Visibility: Science and regulation, *J. Air Waste Man. Assoc.*, *52*, 628-713, 2002.

Wilson, K.R., M. Jimenez-Cruz, C. Nicolas, L. Belau, S.R. Leone, and M. Ahmed, Thermal vaporization of biological nanoparticles: fragment-free vacuum ultraviolet photoionization mass spectra of tryptophan, phenylalanine-glycine-glycine, and beta-carotene, *J. Phys. Chem. A*, *110* (6), 2106-2113, 2006.

Woods, E., III, G.D. Smith, Y. Dessiaterik, T. Baer, and R.E. Miller, Quantitatiave detection of aromatic compounds in single aerosol particle mass spectrometry, *Anal. Chem.*, *73* (10), 2317-2322, 2001.

Zhang, Q., M.R. Alfarra, D.R. Worsnop, J.D. Allan, H. Coe, M.R. Canagaratna, and J.L. Jiménez, Deconvolution and quantification of hydrocarbon-like and oxygenated organic aerosols based on aerosol mass spectrometry, *Environ. Sci. and Technol.*, *39*, 4938-4952 doi:10.1021/es048568l, 2005.

Zhang, Q., J.L. Jiménez, M.R. Canagaratna, J.D. Allan, H. Coe, I. Ulbrich, M.R. Alfarra, A. Takami, A.M. Middlebrook, Y.L. Sun, K. Dzepina, E. Dunlea, K. Docherty, P.F. DeCarlo, D. Salcedo, T. Onasch, J.T. Jayne, T. Miyoshi, A. Shimono, S. Hatakeyama, N. Takegawa, Y. Kondo, J. Schneider, F. Drewnick, S. Borrmann, S. Weimer, K. Demerjian, P. Williams, K. Bower, R. Bahreini, L. Cottrell, R.J. Griffin, J. Rautiainen, J.Y. Sun, Y.M. Zhang, and D.R. Worsnop, Ubiquity and dominance of oxygenated species in organic aerosols in anthropogenically—influenced Northern Hemisphere midlatitudes, *Geophys. Res. Lett.*, *34*, L13801, doi:10.1029/2007GL029979, 2007.

Zhang, X., K.A. Smith, D.R. Worsnop, J. Jiménez, J.T. Jayne, and C.E. Kolb, A Numerical Characterization of Particle Beam Collimation by an Aerodynamic Lens-Nozzle System. Part 1, An Individual Lens or Nozzle, *Aerosol Sci. Tech.*, *36* (5), 617-631, 2002.

Aerosol Science and Technology
Publication details, including instructions for authors and subscription information:
http://www.informaworld.com/smpp/title~content=t713656376

Demonstration of a VUV Lamp Photoionization Source for Improved Organic Speciation in an Aerosol Mass Spectrometer

First Published on: 01 September 2007
To cite this Article: Northway, M. J., Jayne, J. T., Toohey, D. W., Canagaratna, M. R., Trimborn, A., Akiyama, K. I., Shimono, A., Jimenez, J. L., DeCarlo, P. F., Wilson, K. R. and Worsnop, D. R. (2007) 'Demonstration of a VUV Lamp Photoionization Source for Improved Organic Speciation in an Aerosol Mass Spectrometer', Aerosol Science and Technology, 41:9, 828 - 839
To link to this article: DOI: 10.1080/02786820701496587
URL: http://dx.doi.org/10.1080/02786820701496587

Aerosol Science and Technology, 41:828–839, 2007

ISSN: 0278-6826 print / 1521-7388 online
DOI: 10.1080/02786820701496587

Demonstration of a VUV Lamp Photoionization Source for Improved Organic Speciation in an Aerosol Mass Spectrometer

M. J. Northway,[1] J. T. Jayne,[1] D. W. Toohey,[2] M. R. Canagaratna,[1] A. Trimborn,[1] K.-I. Akiyama,[3] A. Shimono,[4] J. L. Jimenez,[5,6] P. F. DeCarlo,[2,6] K. R. Wilson,[7] and D. R. Worsnop[1]

[1]*Aerodyne Research, Inc., Billerica, Massachusetts, USA*
[2]*Department of Atmospheric and Oceanic Sciences, University of Colorado, Boulder, Colorado, USA*
[3]*Japan Automobile Research Institute, Ibariki, Japan*
[4]*Sanyu Plant Service Co., Ltd., Kanagawa-ken, Japan*
[5]*Department of Chemistry and Biochemistry, University of Colorado, Boulder, Colorado, USA*
[6]*Cooperative Institute for Research in the Environmental Sciences (CIRES), University of Colorado, Boulder, Colorado, USA*
[7]*Chemical Sciences Division, Lawrence Berkeley National Laboratory, Berkeley, California, USA*

In recent years, the Aerodyne Aerosol Mass Spectrometer (AMS) has become a widely used tool for determining aerosol size distributions and chemical composition for non-refractory inorganic and organic aerosols. All AMSs to date have used a combination of flash thermal vaporization and 70 eV electron impact (EI) ionization. However, EI causes extensive fragmentation and mass spectra of organic aerosols are difficult to deconvolve because they are composites of the overlapping fragmentation patterns of a multitude of species. In this manuscript we present an approach to gain more information about organic aerosol composition by employing the softer technique of vacuum ultraviolet (VUV) ionization in a Time-of-Flight AMS (ToF-AMS). Our novel design allows for alternation between photoionization (PI) and EI within the same instrument on a timescale of minutes. Thus, the EI-based quantification capability of the AMS is retained while improved spectral interpretation is made possible by combined analysis of the complementary VUV and EI spectra. PI and EI spectra are compared for several compounds and mixtures in multiple dimensions including size distributions and size-segregated mass spectra. In general, VUV spectra contain much less fragmentation than EI spectra and for many compounds the parent ion is the base peak in the VUV spectrum. Results for oleic acid are compared to experiments conducted using tunable VUV radiation from a synchrotron source and were shown to be comparable under similar conditions of photon energy and vaporizer temperature. Future technical modifications for improvements in sensitivity and its potential for ambient measurements will be discussed.

INTRODUCTION

Atmospheric aerosols are well known to affect human health, visibility, ecosystems and agriculture, and climate (Dockery et al. 1997; Watson 2002; NAPAP 1991; IPCC 2001). Organic aerosols compose up to 50% of all fine particulate matter below 2.5 μm in diameter ($PM_{2.5}$) in urban areas, and under many circumstances organic material may account for the majority of the ambient aerosol mass (Kanakidou et al. 2005). It is now widely surmised that organic aerosols contain hundreds to thousands of organic compounds in many chemical classes including alkanes, aldehydes, aromatics, acids, and oligomers (Kalberer et al. 2004; Hamilton et al. 2004). Of this organic aerosol mass, only a small fraction has been compositionally resolved, and much of the organic aerosol mass remains uncharacterized to this date. This lack of knowledge represents an important uncertainty in the role of anthropogenic activities on the future climate and on human health effects, and requires new approaches for the analysis of organic compounds (Murphy 2005).

Aerosol mass spectrometry is a growing area of focus for aerosol speciation because of the wealth of information it can provide on a wide variety of chemical classes in real time.

Received 27 November 2006; accepted 6 June 2007.

The authors wish to thank Silke Hings and Frank Drewnick, and Jose Jimenez's research group for help with ToF-AMS software analysis, and Dr. Tom Baer for useful discussions. Financial support for ARI was provided by two grants from the Department of Energy (DOE) SBIR program (Phase 1 and 2). Part of this work was supported by the Director, Office of Energy Research, Office of Basic Sciences, Chemical Sciences Division of the U.S. Department of Energy under contract No. DE-AC02-05CH11231. PFD and JLJ thank NCAR/UCAR grant 505-39607 and NSF CAREER grant ATM-0449815 for funding for data acquisition software development.

Address correspondence to Megan J. Northway, 45 Manning Rd., Billerica 01821, MA, USA. E-mail: mnorthway@aerodyne.com

Aerosol mass spectrometers generally detect particles through either a single-step particle vaporization/ionization process (laser ablation) (Murphy and Thomson 1995; Noble and Prather 2000; Hinz et al. 1996), or a two-step vaporization/ionization process using a combination of laser desorption/thermal vaporization and various ion detection methods (Jayne et al. 2000; Woods III et al. 2001). The mass spectra of ambient aerosol (particularly organic aerosol) obtained with these instruments are generally complex due to the extensive fragmentation caused by the high-energy ionization methods used.

The Aerodyne Aerosol Mass Spectrometer (AMS) is widely used for obtaining both quantitative chemical composition and size information for aerosols in real-time with no need for preconcentration of samples (Jayne et al. 2000; Canagaratna et al. 2006). The standard AMS uses a combination of flash vaporization, electron impact ionization, and either quadrupole or time-of-flight mass spectrometry to detect fragment ions of the non-refractory component of aerosol particles. Since 70 eV electron impact is universal and inherently linear, its use within the AMS provides quantification and broad detection capabilities. A drawback of the combined flash vaporization and EI ionization detection scheme of the AMS is that it results in extensive fragmentation of organic molecules and limits its organic speciation capability. A deconvolution technique has been developed recently to estimate the mass concentrations and size distributions of hydrocarbon-like and oxygenated organic aerosols in ambient air using an iterative custom principal component analysis method where the time series of m/z 57 and 44 are used as "first order" tracers for fresh "hydrocarbon-like" and oxygenated organic aerosols, respectively (Zhang et al. 2005). Further refinements of this method using the Positive Matrix Factorization (PMF) method offer promise for extracting a few more components from AMS EI data. Since organic aerosols consist of hundreds to thousands of individual chemical species, however, more specific information about the organic species in the aerosol is of great interest.

Less energetic, soft ionization methods, such as single photon ionization (SPI) with VUV light have been shown to simplify the complexity of organic mass spectra in both gas-phase and aerosol phase mixtures (Sykes et al. 2002; Öktem et al. 2004; Mühlberger et al. 2002; Butcher et al. 1999). Resonance-enhanced multi photon ionization (REMPI) is a related soft ionization technique that is highly sensitive, but generally suitable only for (UV absorbing) aromatic components of organic aerosols (Heger et al. 1999; Mühlberger et al. 2001; Cao et al. 2003). Single photon ionization is a more quantitative and linear technique and therefore is more promising for the analysis of gaseous species from the thermal vaporization of aerosol beams. The use of relatively bulky and complex laser systems for the production of pulsed VUV light, in many of these experiments, however, complicates the deployment of such instruments in the field.

Recently, several new sources of VUV radiation have been developed as alternatives to lasers. Low-pressure lamps filled with noble gases and excited by microwave or radio frequency discharge, provide a simple means for a stable, continuous source of VUV photons that may be used to ionize a vapor plume of organic molecules. Nearly all of the organic compounds have ionization energy bands lying within the energy range 8–11 eV, making rare gas lamps ideal light sources for detection of organic molecules (Butcher et al. 1999). In recent mass spectrometry studies, lamp sources with photon intensities on the order of 10^{13}–10^{14} photons sec^{-1} have been reported (Hanold et al. 2004; Kurabuyashi et al. 2005). In other studies, a rare gas lamp pumped with electrons was used to provide a focused source of VUV photons at the excimer emission lines (Mühlberger et al. 2005a, 2005b). Most recently, this lamp was used to examine urban aerosol species desorbed from a filter using a combination of thermal pyrolysis and photoionization time-of-flight mass spectrometry (Streibel et al. 2006).

In this manuscript we characterize a developmental VUV lamp-based photoionization module that can be used together with electron impact (EI) ionization within an Aerodyne Aerosol Mass Spectrometer to provide improved analysis of organic components. We present our experimental design of a compact, robust field-deployable VUV module that is compatible with the current AMS and the first results from the technique. The complementary information provided by the EI and photoionization (PI) spectra for both bulk aerosol and size-segregated aerosol is illustrated for a number of pure and mixed organic aerosol particles. Lastly, the results from the VUV module are closely compared to similar experiments conducted using the tunable VUV radiation at the Advanced Light Source in Berkeley, California. The sensitivities and limits of detection of this method and its potential application for real-time organic aerosol analysis are discussed.

EXPERIMENTAL SECTION

1. ToF-AMS

The Aerodyne Aerosol Mass Spectrometer (AMS) has been described in detail elsewhere (Jayne et al. 2000; Canagaratana et al. 2006). For this study the newly developed time-of-flight (TOF) version of the AMS (referred to as the ToF-AMS) was used, where the traditional quadrupole mass spectrometer has been replaced by a compact orthogonal extraction time-of-flight mass spectrometer (Tofwerk AG, Thun, Switzerland) (Drewnick et al. 2005). The ToF-AMS instrument and the high-resolution version of the same instrument have been described previously (DeCarlo et al. 2006); hence, only the relevant details are described here.

As in the case of the quadrupole AMS, aerosol particles are sampled into the ToF-AMS using an aerodynamic lens (Zhang et al. 2002). The particles exit the lens and pass through a 1 mm i.d. channel skimmer, which skims most of the remaining air and transmits the particle beam into the aerosol-sizing chamber (pressure $\sim 1 \times 10^{-5}$ Torr). In this expansion, the particles achieve a terminal velocity depending on their vacuum

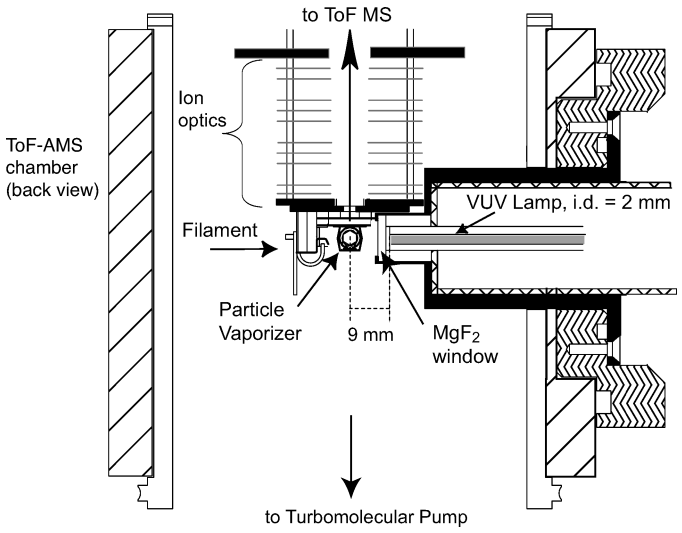

FIG. 1. Cross-sectional view of the VUV module and ionization region of the Aerodyne ToF-AMS. The particle beam is coming into the page.

aerodynamic diameters (DeCarlo et al. 2004). The particle beam next encounters a rotating mechanical chopper (chopper cycle, 150 Hz, effective duty cycle 2%) that produces pulses of particles, the phasing of which is used to determine particle diameters based on variable particle flight times. After the particles travel through the aerosol sizing chamber they impact on a heated tungsten vaporizer ($\sim$600°C) and all non-refractory components of the aerosol vaporize. As the particle is rapidly vaporized, the vapor plume is immediately ionized via electron impact with 70 eV electrons emitted by a tungsten filament.

Ions are extracted into the ToF-AMS with a pulse rate of 83.3 kHz, over a variable mass range from 1 to 1000 amu. When using a mass range of 0 to 300 amu, acquisition of one mass spectrum takes less than 12 μsec. As this time scale is much less than that of a chopper cycle (150 Hz), multiple mass spectra are obtained for each particle size, and even mass spectra of individual particles are possible. At these conditions and including the necessary dead times in the data acquisition system, typically about 500 spectra are taken for each chopper cycle. Ions are detected with a chevron-style multi-channel plate (MCP) detector (Burle Technologies, Sturbridge, MA). An important feature of the ToF-AMS is the high-speed (1Gs/s) analog-to-digital converter data card (AP240, Acqiris, Geneva, Switzerland). This board allows for the averaging of raw mass spectra in real time before transfer to a PC for storage. In addition, the AP240 allows for the user to input a noise "threshold" below which all data are discarded. The threshold is set above the electronic noise level, but below the average signal peak height for a single ion. This allows for discrimination of ions as single events, and their temporal distributions reflects Poisson ion counting statistics. Because of the relatively low signals in the VUV ionization mode in comparison to the electron impact mode, this discrimination is critical for the improving the signal-to-noise levels and results in the adequate signals in minutes.

2. VUV Ionization Module

A cross section of the modified AMS ionization region is shown in Figure 1. In the typical AMS systems only one filament is run at a time, but two filaments are present to avoid the need to vent the instrument if the filament in use fails. To operate in VUV mode, one of the two filaments is removed and replaced with the VUV lamp assembly. The assembly, consisting of an adapter flange, a stainless steel/window housing, and a module containing the VUV lamp and associated electronics, mounts to an existing port on the vacuum chamber, allowing for direct access to the ionization region. The entire assembly weighs about 3 kg with dimensions of 20 mm $\times$ 10 mm $\times$ 8 mm. The stainless steel window housing contains an MgF_2 window (TMS Vacuum Components, East Sussex, England) such that the lamp is operated at atmospheric pressure, but the VUV photons are transmitted through the MgF_2 into the high vacuum of the ionization region. The lamp itself is custom made by filling a quartz tube with $\sim$1–3 Torr of Krypton gas and a chemical getter (Barium metal) and sealing it with an MgF_2 window. During operation, a low flow of N_2 is continually introduced to purge any space between the two MgF_2 windows and avoid absorption of the VUV light from atmospheric oxygen. The VUV light is initiated by a high voltage discharged and maintained by a solenoidally coupled 180-MHz radiofrequency discharge powered by a $\sim$5–10 W single-stage oscillator/amplifier.

Figure 2 shows a typical spectrum of a VUV lamp, with two strong emission lines at 10 and 10.6 eV, (123.6 nm and 118.0 nm, respectively). These wavelengths are emitted as a result of the decay of collisionally excited Kr atoms created by the RF-discharge. Each lamp is about 5 cm long with an o.d. of 6 mm and an i.d. of 2 or 3 mm. Thus, the useful portion of the plasma is contained within the small volume adjacent to the window. The photon intensity at the exit of the Krypton lamp of the VUV module is estimated to be 5×10^{13} photons sec^{-1}. This

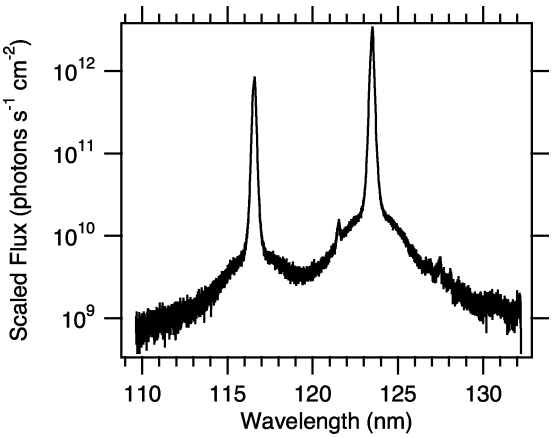

FIG. 2. VUV spectrum of a typical Krypton lamp used here, showing the two atomic line emissions at 116.5 nm (10.6 eV) and 123.6 nm (10 eV).

estimate, which is likely only accurate within a factor of 4, was obtained by exposing a phototube (Hamamatsu, Shizuoka-ken, Japan) to the lamp and measuring its direct current output after amplification with an analog current amplifier. The average photocathode activity over the entire surface specified by the manufacturer (12 mA/Watt at 121.6 nm) was used in the estimation. Using this value and the active area of the plasma, the total flux at the immediate lamp exit was calculated to be 5×10^{14} photons sec^{-1} cm^2. The absolute values shown in Figure 2 have been scaled to reflect this total flux value.

As shown in Figure 1, when the VUV module is connected to the ToF-AMS, the photons enter the ionizer through a 3 mm diameter aperture on its side. The light lost due to this baffling was simulated by placing a 3 mm mask in front of the phototube. From these experiments it was estimated that the VUV beam divergence is about 2 mm per 10 mm (~0.10 steradians), resulting in a light output at the exit of the lamp of 5×10^{14} photons sec^{-1} $steradian^{-1}$. This lamp brightness is similar to those quoted for commercially available VUV lamps with similarly sized plasma volumes. Including both the $1/r^2$ losses and the baffling effect, the total number of photons reaching the ionizer is estimated to be about 2×10^{13} photons sec^{-1}. For reference about 1.5×10^{16} electrons (2.5 mA) are emitted from the filament in the EI AMS.

3. Aerosol Generation

Laboratory aerosols were generated one of two ways. The first method was to dissolve a small amount of sample in a solvent and use a constant output collision atomizer (TSI Inc. Model 3076, St. Paul, MN) to generate a polydisperse sample of pure aerosol with a size mode between 10–1000 nm with a peak at ~100 nm. Pristane was dissolved in dichloromethane, atomized, and dried through a tube filled with activated charcoal. The second method, used generally for oleic acid, was to nucleate aerosols homogeneously by heating a bath of the pure compound and subsequently creating a supersaturation by cooling the air. The cigarette smoke aerosol was sampled in the laboratory as a sidestream measurement with the AMS inlet. This mixture was sampled "in situ" with no pre-concentration.

4. Synchrotron Measurements

To further characterize the VUV photoionization module, a number of experiments were conducted with the AMS at the Chemical Dynamics Beamline of the Advanced Light Source (ALS) at the Lawrence Berkeley National Laboratory. The synchrotron VUV light is generated from an undulator and can be continuously tuned from 7 to 25 eV. The source delivered a highly polarized photon beam of $\sim 10^{16}$ photons sec^{-1} with a spot size of approximately 1 mm (horizontal) by 0.2 mm vertical directly into the ionization region of the AMS. The AMS was coupled to the light source using a similar set-up to that shown in Figure 1, where the light beam entered the ionization region of the AMS through a vacuum flange on the side of the instrument. The alignment of the beam in the AMS ionizer was carefully tuned by both visual alignment using a window and by minute adjustments of the position of the instrument relative to the photon beam.

RESULTS AND DISCUSSION

1. Comparisons of EI and PI spectra

Figure 3 shows a comparison of electron impact and photoionization mass spectra for pristane (IUPAC name = 2,6,10,14-tetramethylpentadecane). Pristane is a simple, highly branched alkane, which is representative of a hydrocarbon-like mass spectrum with a high fraction of small alkyl fragments. The spectrum in Figure 3a highlights the extensive fragmentation that is typically observed in AMS EI spectra for this type of organic species. The EI spectrum is dominated by ions that result from secondary fragmentation of the primary ion fragments (m/z 113, m/z 183, and m/z 253) of pristane (McLafferty and Turecek 1993). These secondary ions, at m/z 43, 57, and 71, are commonly observed ions for EI spectra of alkanes. The molecular ion at m/z 268 is not visible on a linear scale in the EI spectrum. Although the PI spectrum also contains the ions at m/z 43, 57, and 71, it shows clearly the primary fragments and a prominent peak at the pristane molecular ion on a linear scale. Thus, the PI spectrum provides more specific information about the pristane parent molecule than the EI spectrum.

Figure 4 shows EI and PI spectra for cigarette smoke, which is a rich mixture of unsaturated aliphatic hydrocarbons, carboxylic acids, PAHs, and oxygen and nitrogen heterocyclic aromatic compounds (Rogge et al. 1994). Overall, the photoionization spectrum differs from the EI spectrum in that it contains many high mass fragments above m/z 100 that are visible on the linear scale, including some above m/z 400. Previous studies of cigarette smoke particles reported that although nicotine is a fairly volatile compound, it is an abundant compound found in cigarette smoke particles (Rogge et al.

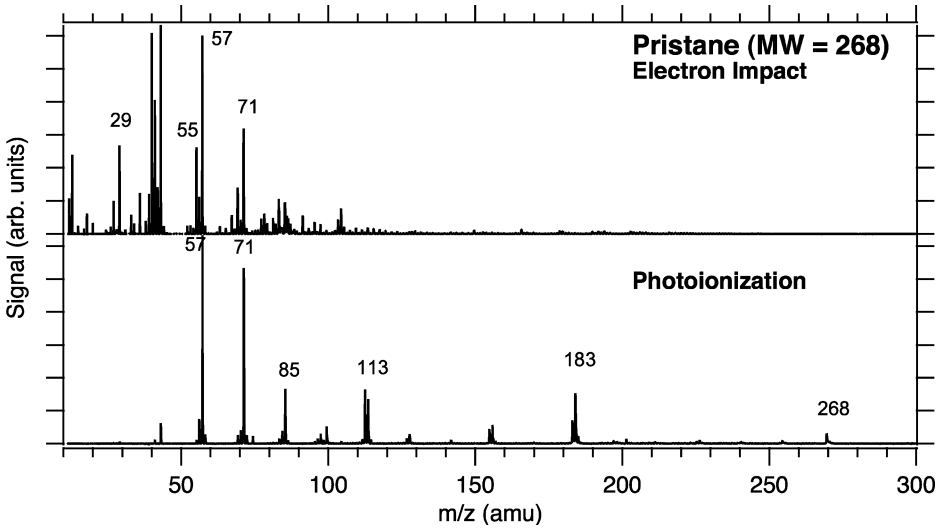

FIG. 3. Comparison of ionization techniques for pristane particles.

1994). The molecular mass of nicotine, m/z 162, is a prevalent peak in the PI spectrum, but not in the EI spectrum. The m/z 84 fragment ion, which dominates the PI spectrum and is present in the EI spectrum, corresponds to another nicotine fragment (NIST 2005). Although there is signal at almost every peak out to about m/z 400, many of the most dominant peaks are found to be consistent with organic molecules identified in GC/MS studies on cigarette particles that make up approximately 27% of the measured organic mass (Rogge et al. 1994). The peaks at m/z values 95 and 146, for example, may correspond to the molecular ions of 3-hydroxypyridine and myosmine which are two heterocyclic nitrogen-containing compounds generally found in large amounts in cigarette smoke particles. The large peak at m/z value 110 could similarly result from the molecular ion of any of the dihydroxybenzenes such as 1,2-dihydroxybenzene (catecol), 1,3-dihydroxybenzene (resorcinol) or 1,4-dihydroxybenzene (hydroquinone) (Pers. Comm. A. Shimono; Rogge et al. 1994). Similarly, the peak at m/z 124 may result from 3- or 4-methyl catecol, which are noted carcinogens also present in side stream measurements (Pers. Comm. A. Shimono). The hydrocarbon series of high mass peaks at m/z values 380, 394, 408, 422, and 436 is consistent with long chain hydrocarbons (C27-C31), which have been found in high loadings in cigarette smoke. The peaks at m/z 178 and m/z 202 are indicative of PAH species anthracene/phenanthrene and pyrene/fluoranthene respectively. Since the PAHs are typically resistant to fragmentation, they are observed as parent ions in both the EI and PI spectra. Because cigarette smoke is such a rich mixture of hundreds of compounds, these peak assignments are tentative, but this type of analysis illustrates the way in which

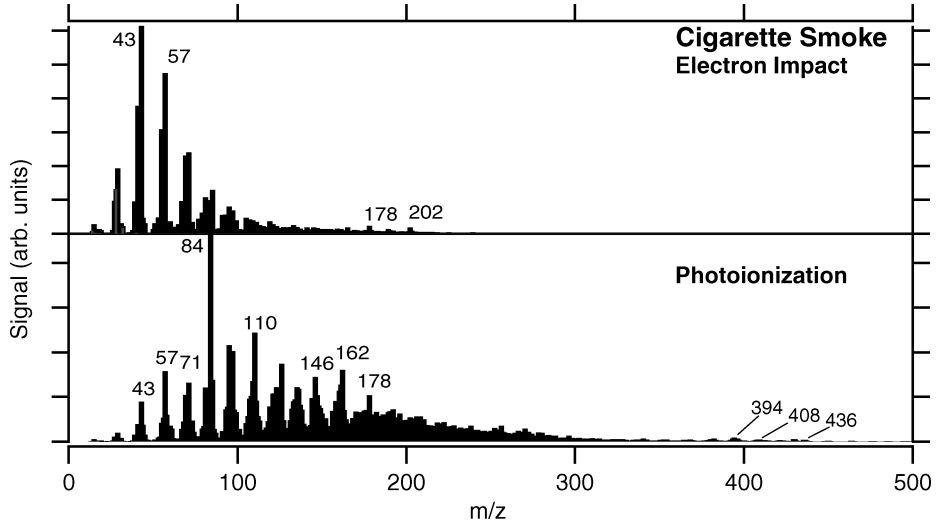

FIG. 4. Comparison of electron impact and VUV ionization mass spectra for cigarette smoke.

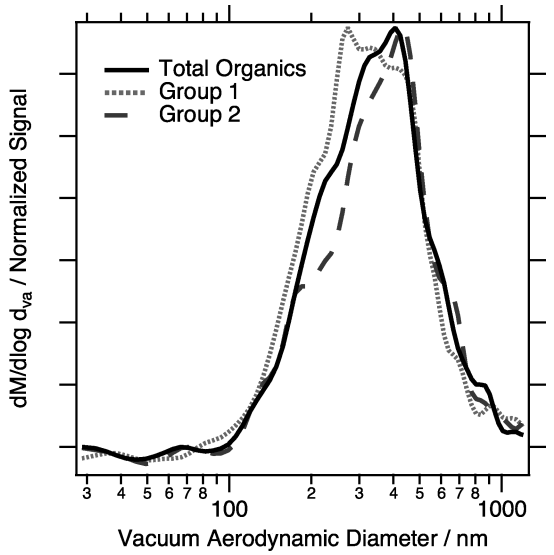

FIG. 5. VUV photoionization normalized size distributions from cigarette data for total organics (black line) and the weighted average of selected m/z values (tentative compound assignments from text in parentheses) for Group 1 (gray dotted line): 110 (dihydroxybenzenes) and 146 (myosmine), and Group 2 (dark gray dashed line): m/z 84 (nicotine fragment), 95 (hydroxypyridine), 162 (nicotine), and 178 (anthracene/phenanthrene).

PI spectra can enhance the chemical speciation capability of the AMS.

Links between aerosol chemical composition and aerosol size can be used to obtain even more detailed information about organic aerosol sources and processes in the atmosphere. For example, in previous studies chemically speciated size distributions have been used in quadrupole-based AMS studies to differentiate between fresh combustion aerosols and aged oxidized organic aerosols (Alfarra et al. 2004; Jayne et al. 2000). The ToF-AMS, with either EI or PI ionization, is also capable of providing chemically resolved particle size distributions. Figure 5 shows the average size dependent distribution for the total organic mass and two groups of PI fragments measured while sampling cigarette smoke particles. Group 1 consists of m/z 110 and 146 (likely from any of the dihydroxybenzenes and myosmine, respectively) which peak at around 250 nm. Group 2 consists of nicotine fragments (m/z 162 and 84) and other m/z values that are tentatively assigned to hydroxypyridine (m/z 95) and anthracene/phenanthrene (m/z 178). The latter size distribution peaks near 450 nm. The different size distributions for the two groups of organic ions and fragments clearly indicate that the size distribution observed for the total organic mass has contributions from overlapping modes of different composition.

Since the ToF-AMS instrument provides a complete EI and PI mass spectrum for every size bin, the size dependence of the cigarette smoke particle composition can be examined in more detail. This is demonstrated in Figure 6 which shows PI mass spectra averaged over the size bins 20–350 nm, 350–600 nm, and 600–1200 nm from Figure 5. The PI mass spectra clearly show differences in the aerosol chemical composition with particle size. The smallest size mode is dominated by the m/z value 110, but the middle and largest size modes are dominated by the nicotine fragment (m/z 84), as in the total mass spectrum (Figure 4). The relative importance of the m/z 178 (possibly PAH) also decreases as size increases. As illustrated in Figure 4, PI fragments at high m/z contain significant molecular information; hence, they provide more useful and relevant information about the size dependence of aerosol composition than the chemically-speciated size distributions measured with EI alone. Thus, the combination of PI with chemically resolved size distributions from the ToF-AMS promises to be a powerful tool for examining size-dependent chemical variations in aerosol composition.

2. Optimizing Spectral Information Available with PI

The exact photoionization spectrum (i.e., degree of fragmentation) from a particular compound depends strongly on both the sample temperature (aerosol vaporization method) and the photoionization energy used. Both of these factors can contribute excess energy to the ions and may result in additional fragmentation of the molecular ion. Previous studies have shown that the degree of fragmentation can be reduced by using lower vaporization temperatures or by using lower photon energies (Nash et al. 2005; Wilson et al. 2005; Mysak et al. 2005). For example, for the compound oleic acid, researchers have obtained VUV spectra with very little fragmentation (Mysak et al. 2005). In order to study the exact fragmentation observed using our system, spectra of oleic acid were taken under a number of varying conditions. Figures 7a and 7b show the EI and PI spectra for oleic acid taken with the vaporizer at 500°C, standard operating conditions for EI. Since oleic acid has a backbone that consists of a long chain alkane, its EI spectrum has many secondary fragments that are the same as in the pristane spectrum (Figure 3). The PI spectrum of oleic acid, on the other hand, shows significant differences not only from the oleic acid EI spectrum but also from the pristane PI spectrum. Figure 7c shows the same photoionization spectrum of oleic acid particles taken with the AMS vaporizer temperature at 200°C. When compared to Figure 7b, it is clear that the extent of fragmentation is highly dependent on the internal energy of the molecules prior to ionization. In Figure 7c, relative to the molecular ion (m/z 282) the intensity of the fragment ions (particularly at m/z 84, 98, and 111) has decreased with decreased AMS vaporizer temperature, and the m/z 264 is now the highest peak in the spectrum. The ion fragment at m/z 264 results from the loss of the water ion from the parent ion, likely from thermal decomposition of the molecule upon vaporization and not from a ion fragmentation process, and is thus a surrogate for the molecular ion of oleic acid. Thus, it may be inferred that a significant amount of fragmentation can be avoided by using vaporizer temperatures just above the boiling point (or thermal decomposition point) of the compounds of interest. However, in most cases, such as in sampling atmospheric aerosol, there will be many organic compounds present in the aerosol, and

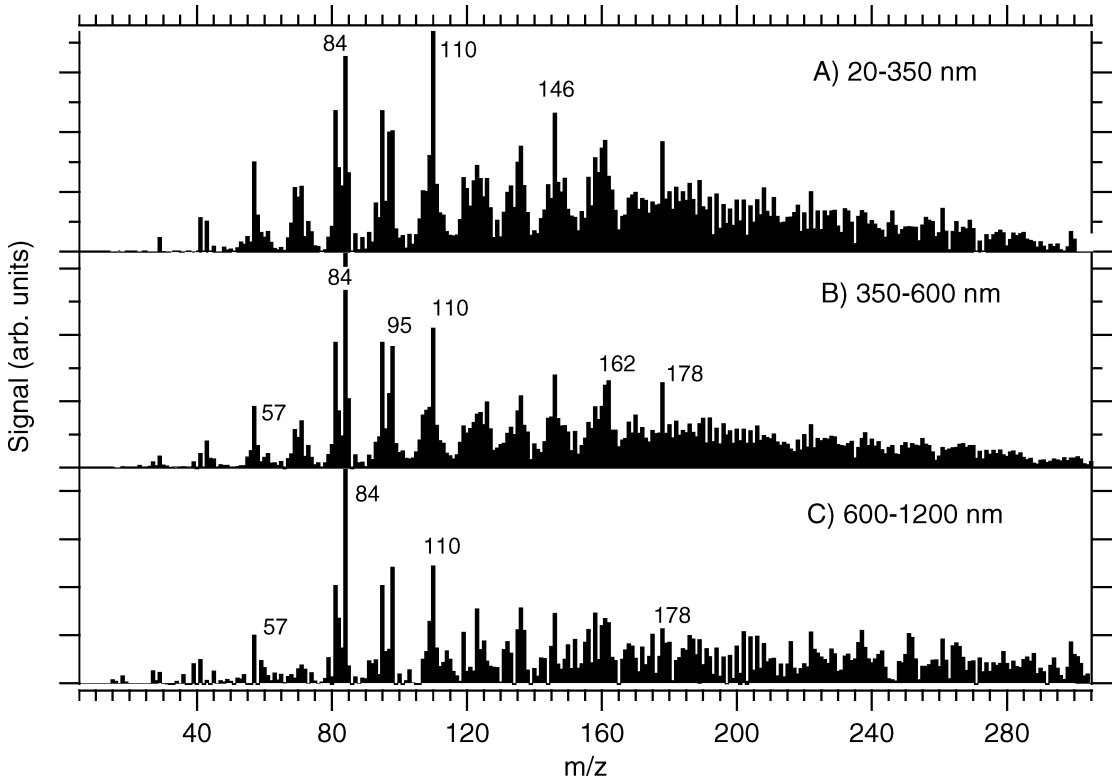

FIG. 6. Size-segregated mass spectra for the cigarette smoke particles shown in Figures 4 and 5. Size bins are labeled as (a) 20–350 nm, (b) 350–600 nm, and (c) 600–1200 nm.

therefore optimizing the temperature for minimal fragmentation for all compounds is not possible.

One complication that arises when acquiring PI spectra is unintended electron impact ionization that results from photoelectrons that are formed in the ionization region (Mühlberger et al. 2005a). Photoelectrons are produced in the ionization region by photons striking the metal surfaces of the ionizer. As they are typically formed, these photoelectrons have sufficient energy to ionize the air, water, and oxygen molecules (ionization energies of 12–14 eV) that are present as gas phase molecules in the focused molecular beam but are not photoionized by 10.6 eV VUV photons. Thus, the presence of these signals is indicative of photoelectron impact occurring in the ionization region. When aerosol signals are small ($<10\ \mu g\ m^{-3}$) these air peaks are sometimes the largest in the mass spectrum. When photoelectrons are present, electron impact ionization also occurs for vaporized aerosol molecules. For example, the presence of some inorganic aerosol signals in the ambient mass spectrum, such as ammonia and nitrate, is another indication of photoelectrons in the system. Moreover, for any given compound, the presence of photoelectrons will generally cause much more fragmentation of the molecular ion than in pure photoionization, causing the mass spectrum to look more like an electron impact spectrum.

The number of photoelectrons can be reduced by minimizing the metal surface area in the system that is exposed to stray and diverging photons from the lamp. We have attempted to do this in our system by positioning the lamp as close as possible to the ionization region of the AMS, thereby minimizing $1/r^2$ divergence of photons from the lamp. The improved design brought the lamp 5 mm closer to the ionizer and reduced the number of photoelectrons by an estimated factor of 20–50. This design also improved the photon delivery to the ionization region by a factor of 2, resulting in a corresponding increase in sensitivity. The N_2^+ and O_2^+ signals from photoelectrons were also reduced by a similar factor. Figures 7c and 7d show a comparison of the photoionization of oleic acid particles at 200°C using the initial and modified designs of the VUV module. Although the spectra are very similar above 150 amu, the spectrum from the new VUV interface design shows a dramatic decrease in the relative intensity of the fragment ions below m/z 100, indicating reduced electron impact. In particular the fragment ions at m/z 43, 55, and 69 seem to be mostly generated by electron impact and are much reduced ($\sim\times$20–50), which is consistent with the reduction in photoelectrons in the new design. In order to quantify the extent to which the electron impact ionization was reduced in the improved VUV module, the oleic acid spectra discussed above were compared with similar experiments carried out at the Advanced Light Source in Berkeley, CA. The synchrotron photon beam was delivered to the AMS in an analogous manner to the VUV lamp module in standard operation. However, because

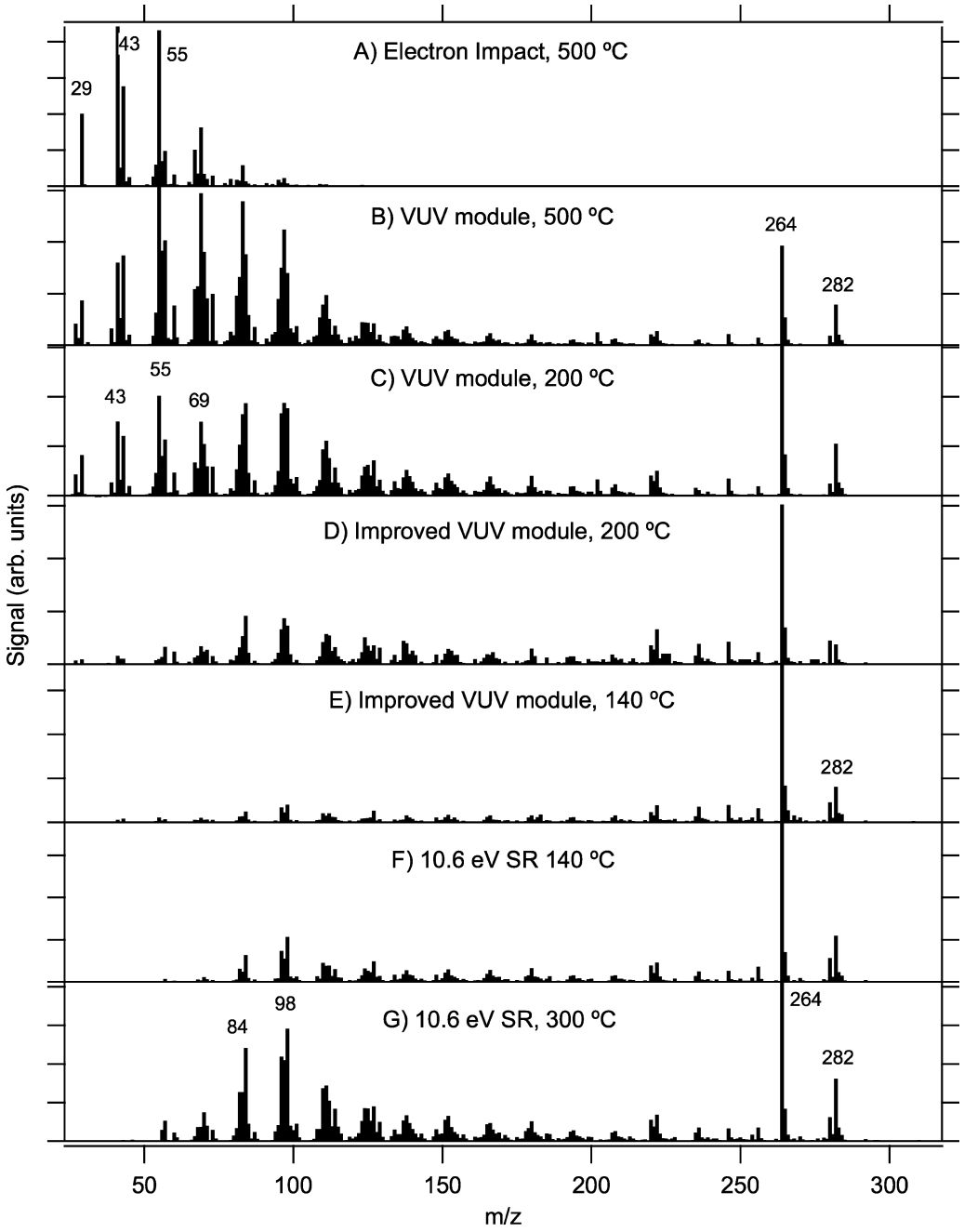

FIG. 7. Comparison of spectra of oleic acid aerosol taken at varying conditions: (a) EI spectrum with vaporizer at 500°C. (b) VUV module with vaporizer at 500°C. (c) VUV module with vaporizer at 200°C. (d) 200°C using improved VUV module (e) 140°C using improved VUV module. (f) 140°C using synchrotron radiation at 10.6 eV g) 300°C using synchrotron radiation at 10.6 eV.

the diameter of the synchrotron photon beam is much smaller than the entrance aperture into the AMS ionizer, the possibility of photoelectron production and electron impact contamination using this source was nearly zero. Figures 7e and 7f show the oleic acid spectrum using the improved VUV module and the synchrotron radiation at 10.6 eV both taken at an AMS vaporizer temperature of 140°C. Indeed a visual comparison of these two spectra shows a striking similarity, suggesting that most of the electron impact has been removed in the improved VUV module. Figure 7g shows the oleic acid PI spectrum taken using the synchrotron radiation at 10.6 eV at an AMS vaporizer temperature 300°C. Note that the fragmentation at 300°C (7g) using the pure photoionization from the SR is notably different from the fragmentation at 200°C using the old VUV module (7c),

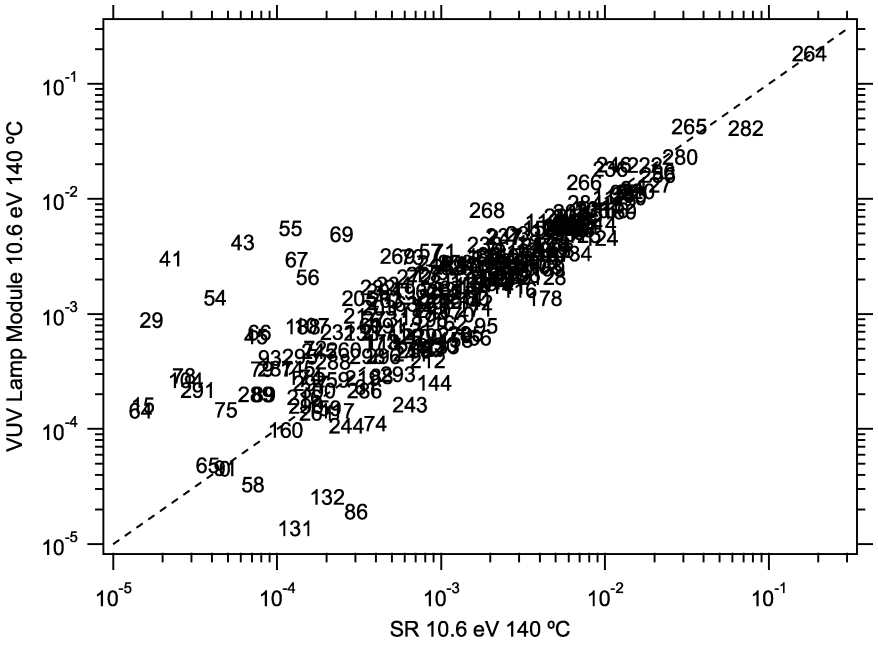

FIG. 8. Correlation plot comparing mass spectra taken using VUV lamp module (Figure 7e) and the synchrotron radiation (Figure 7f), both at 140°C.

providing evidence that much of the fragmentation in 7c is due to electron impact ionization and not excess thermal energy. In particular, the fragments at m/z 84 and 98 are increased from the excess thermal energy, but not those at m/z 43, 55, and 69. Finally, Figure 8 shows a scatter plot of the mass spectra from Figures 7e and 7f, indicating good agreement between the two spectra. The fragment ions that notably fall off the line, m/z 43, 55, and 69, are likely mostly due to the small amount of photoelectron impact ionization that still remains in our system. However, as shown in the normalized log plot, these fragments are less than 0.01% of the total signal, suggesting that the photoelectrons in our system have been reduced to a nearly negligible level.

Figure 9 shows the results of synchrotron experiments that mapped the PI spectra of oleic acid as a function of VUV energy and AMS vaporizer temperature. The ratio of the molecular ion and base peak sum (m/z 282 + m/z 264) to the total ion signal (designated M^+/Total Ion) is maximized for all temperatures near the ionization energy of 8.7 eV (Mysak et al. 2005). At this point and the lowest temperatures, more than 75% of the signal is in the parent ion signal. As expected, increased AMS vaporizer temperature causes an increase in fragmentation at all energies above the ionization energy. However, the value of M^+/Total Ion reaches a maximum for all profiles around 100°C. Below this temperature there is very little excess thermal energy, however near this temperature the total signal does begin to decrease and vaporization of the oleic acid aerosol is presumably no longer a "flash vaporization" process. Thus, for soft ionization in the AMS it is important to find an optimum temperature where all of particles are vaporized, but thermal fragmentation is still minimized.

3. Sensitivity and Limits of Detection

The ionization efficiency in the AMS with the EI or PI process can be expressed as:

$$IE = \sigma \cdot F \cdot \tau \cdot E \qquad [1]$$

where σ is the appropriate ionization cross-section of the molecule of interest, F is the ionizing photon or electron flux, τ is the residence time available for ionization, and E is the ion transmission and detection efficiency of the mass spectrometer.

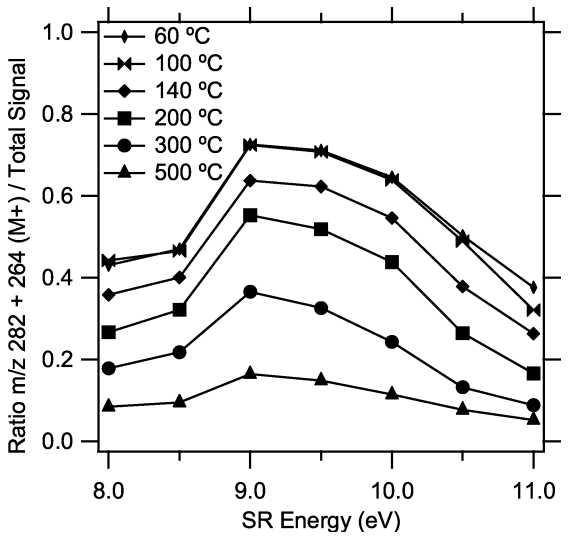

FIG. 9. Temperature and VUV photon energy dependence for photoionization of oleic acid using synchrotron radiation.

Thus, for a given mass spectrometer where τ and E do not vary, the relative IE for electron impact compared with photoionization can be expressed as:

$$IE_{EI}/IE_{PI} = (\sigma_{EI}/\sigma_{PI}) \cdot (F_{EI}/F_{PI}). \quad [2]$$

In general, for organic molecules the cross-sections for photoionization are 20–70 times smaller than the cross-sections for electron impact ionization (Cool et al. 2003; Berkowitz 2002; Jimenez et al. 2003). During EI ionization, the AMS ionizer usually operates at an emission current of 2.5 mA, which corresponds roughly to an output of 1.5×10^{16} electrons sec^{-1}. Since the evaporative plume produced by flash heating of a particle is confined by the ionizer geometry and is much smaller than the volume of light from the lamp (or electrons from the filament in the case of EI), the ionizing volume for both processes is assumed to be the same, and the value of F_{EI} /F_{PI} is approximately equal to the ratio of electron output to photon output for the two processes (units of photons sec^{-1} or electrons sec^{-1}). As discussed in the Experimental section, the VUV lamp yields an output of 2×10^{13} photons sec^{-1} at the ionizer, such that the value of F_{EI} /F_{PI} is 500. Thus taken together, according to equation 2, the IE_{EI}/IE_{PI} is estimated to be 1×10^4.

For the both the quadrupole and the ToF-AMS instruments IE_{EI} is routinely measured as a metric of the instrument sensitivity and stability (Jimenez et al. 2003). The calibration procedure involves the use of size-selected particles of known concentration. The IE is defined as the ratio of the average measured number of ions per particle to the known number of molecules per particle. The IE_{PI} has been measured by an analogous procedure for oleic acid. As summarized in Table 1, a typical measured value for IE_{EI} (for 70 eV electron impact) in a ToF-AMS for oleic acid is 1×10^{-6} and the measured IE_{PI} of oleic acid is 2×10^{-10}. The ratio of these measured values, 5000, is within a factor of 2 of the estimated value from Equation (2).

The detection limit in EI mode for organic species in a 1-minute average spectrum is approximately 20 ng m^{-3}(DeCarlo et al. 2006). Because the thresholding feature of the Acqiris data acquisition card can be used to discriminate against electronic noise, the instrument noise can be reduced to simply the dark counts of the MCP. For a new set of MCPs this value can be as low as 1 count per minute, although values of 2–5 counts per second are more typical. For the experiments here, the RMS noise calculated for the difference signal with no particles (filter measurement) is typically around 0.002 bits per extraction, which corresponds to 3 μg m^{-3} for a 1-minute average. Thus, the 3σ limit of detection for oleic acid is calculated to be about 12 μg m^{-3} for a 1-minute average, based on the measured ionization efficiency for this molecule shown in Table 1. This detection limit is ~1000 times, rather than 10,000 worse than for EI due to the ability to further discriminate against noise in the VUV mode by increasing the MCP gain. During EI operation the MCP gain is limited by avoidance of saturation of the large signals, which is not a concern for VUV operation. For some ions (e.g., m/z 43), there is a significant gas-phase background that increases the limit of detection for aerosol signals. Furthermore, at very high particle mass concentrations, ions scattered in the grids of the TOF flight region will arrive at m/z's other than their nominal values, resulting in baseline noise that also will affect the limits of detection. Limits of detection for many other organic molecules will generally be in the 10–12 μg range, depending on the specific photoionization cross section of the molecule. It should be noted that the limits of detection reported here are for a single component aerosol. Thus, the limit of detection must be exceeded for each compound in an aerosol mixture to detect a signal for that compound. This is in contrast to EI, where excessive fragmentation causes ions from different compounds to add, especially in the smaller m/z's, aiding in the detection of total organics.

TABLE 1
Comparison of EI and PI sensitivity parameters

	EI ionization	Photoionization (PI)	EI/PI
Flux, part cm^{-2} sec^{-1}	1×10^{16} /area	2×10^{13}/area	5×10^2
σ,cm^2 $molec^{-1}$	6×10^{-16}	3×10^{-17}	20
Measured IE	1×10^{-6}	2×10^{-10}	5×10^3
Predicted IE_{EI}/IE_{PI}			1×10^4

It is clear from Table 1 that the sensitivity of PI relative to EI can be improved by increasing the photon flux of the VUV lamp. The photon output of the lamp used in these studies is likely within a factor of 10 of its theoretical maximum for an unfocused beam. We believe that the plasma is near saturation for two reasons: first, when the input RF power is increased, the photon flux does not increase. Moreover, other commercially available lamps of the same geometry have similar outputs. For example, Resonance, Ltd, in Ontario, Canada, produces lamps with an output of 3×10^{15} photons $steradian^{-1}$ sec^{-1} for a 12 mm diameter lamp. The effective area of this lamp is 16 times larger than the 3 mm lamp used for the measurements shown in this manuscript, and therefore actually has a very similar output per area or flux as the lamp used here. Therefore, this lamp would not increase the sensitivity of method in the AMS without some way to concentrate the beam.

Other researchers have used different lamp designs to improve photon fluxes, without the use of a laser. Notably, Mühlberger and coworkers have developed the Electron-Beam-Pumped Excimer VUV lamp, whereby a Kr or Ar source is irradiated with electrons from an electron gun to create rare gas excimers (Mühlberger 2005a, 2005b). These excimers decay to produce VUV light that can be a source for single photon ionization. Reported photon intensities are presently about 1.5×10^{13} photons s^{-1}, but are expected to increase by a factor of ten in the near future (Mühlberger et al. 2005a). If indeed such

lamps eventually create more photons than the rare gas lamps of a similar size, they would allow for a sensitivity increase for VUV ionization within the AMS.

Another approach is to use the photons from the VUV lamp not for direct ionization but for the ejection of photoelectrons from a photoemissive surface that is coupled into the AMS. In this method, known as PERCI (Photoelectron Resonance Capture Ionization Mass Spectrometry), the photoelectrons are finely tuned to a low energy (<0.1 eV), by the addition of an extra electrode near the photoemissive surface (LaFranchi et al. 2004). These low energy photoelectrons attach to analyte molecules resulting in little or no fragmentation (LaFranchi et al. 2004). This technique could be a feasible alternative to photoionization in the AMS.

CONCLUSION

This manuscript presents the first results obtained from a field-deployable VUV lamp module that can be interfaced to the Aerodyne Aerosol Mass Spectrometer to provide PI spectra of aerosol chemical species in real time. The results presented here indicate that photoionization using rare gas lamps is a promising ionization technique for improving the molecular information provided by AMS mass spectra. Although the high temperature of the AMS vaporizer induces some thermal fragmentation, the PI spectra are less complex than EI spectra due to decreased fragmentation. The PI spectra obtained from the VUV lamp are similar to those obtained with VUV radiation from a synchrotron source. Comparisons of EI and PI spectra of pure organic aerosols show that the presence of parent peaks and characteristic fragments at masses greater than m/z 100 in the PI spectra provide clearer signatures for chemical identification. Even in more complex organic mixtures such as cigarette smoke particles, the PI spectra provide more information about the molecular composition of the aerosol than EI spectra. Speciated size distributions measured with the PI detection technique offer an additional means of increasing the chemical information that can be obtained by the AMS for complex mixtures of aerosol particles.

The reported PI detection limits of 10–12 μg m$-$3 in a 1-minute sample are sufficient for laboratory work, source sampling, and detection of atmospheric aerosol in polluted urban atmospheres at fixed sites. The PI spectra presented here, however, are limited by photon fluxes in comparison to electron fluxes in electron impact ionization, and span only 3–4 orders of magnitude in signal in comparison to the 7 orders of magnitude spanned by the current AMS in standard electron impact mode. With several ongoing advances in excimer rare gas lamp technology there is a significant potential of improving the sensitivity of the photoionization technique by a factor of 50–100, which would be similar to the existing quadrupole AMS instruments.

A key feature of the VUV lamp module design is its ability to alternate between PI and EI detection on the timescale of minutes. This feature allows for the combination of the advantages of both detection techniques. While PI offers spectral simplicity, alternation of PI with the EI allows for increased sensitivity to organic aerosol mass and maintains the AMS sensitivity to inorganic species like SO_4 and NO_3 which are not effectively ionized by 10.6 eV PI. The ability to alternate PI detection with EI is also important because electron impact ionization efficiency has an empirical dependence on chemical composition and molecular weight that can be readily used to quantify speciated mass.

REFERENCES

Alfarra, M. R., Coe, H., Allan, J. D., Bower, K. N., Boudries, H., Canagaratna, M. R., Jimenez, J. L., Jayne, J. T., Garforth, A. A., Li, S-M., and Worsnop, D. R. (2004). Characterization of Urban and Rural Organic Particulate in the Lower Fraser Valley using Two Aerodyne Aerosols Mass Spectrometers, *Atmos. Env.* 38:5745–5758.

Berkowitz, J. (2002). *Atomic and Molecular Photoabsorption: Absolute Total Cross Sections*. Academic Press, San Diego, 350 pp.

Butcher, D. J., Goeringer, D. E., and Hurst, G. B. (1999). Real-time Determination of Aromatics in Automobile Exhaust by Single-Photon Ionization Ion Trap Mass Spectrometry, *Anal. Chem.* 71:489–496.

Canagaratna, M. R., Jayne, J. T., Onasch, T. B., Williams, L. R., Trimborn, A., Northway, M. J., Kolb, C. E., Worsnop, D. R., Jimenez, J. L., Allan, J. D., Coe, H., Alfarra, M. R., Zhang, Q., Drewnick, F., and Davidovits, P. (2007). Chemical and Microphysical Characterization of Ambient Aerosols with the Aerodyne Aerosol Mass Spectrometer, *Mass Spectrom. Rev.* 26:185–222.

Cao, L., Mühlberger, F., Adam, T., Streibel, T., Wang, H. Z., Kettrup, A., and Zimmermann, R. (2003). *Anal. Chem.* 75:5639–5645.

Cool, T. A., Nakajima, K., Mostefaoui, T. A., Qi, F., McIlroy, A., Westmoreland, P. R., Law, M. E., Poisson, L., Peterka, D. S., and Ahmed, M. (2003). Selective Detection of Isomers with Photoionization Mass Spectrometry for Studies of Hydrocarbon Flame Chemistry. *J. Chem. Phys.* 119(16):8356–8365.

DeCarlo, P., Slowik, J. G., Worsnop, D. R., Davidovits, P., and Jimenez, J. L. (2004). Particle morphology and Density Characterization by Combined Mobility and Aerodynamic Diameter Measurements. Part 1: Theory. *Aerosol Sci. Technol.* 38:1185–1205.

DeCarlo, P. F., Kimmel, J. R., Trimborn, A., Northway, M., Jayne, J. T., Aiken, A. C., Gonin, M., Fuhrer, K., Hovarth, T., Docherty, K. S., Worsnop, D. R., and Jimenez, J. L. (2006). A Field-Deployable High-Resolution Time-of-Flight Aerosol Mass Spectrometer, *Anal. Chem,* 74:8281–8289.

Dockery, D. W., Pope, C. A., Xu, X. P., Spengler, J. D., Ware, J. H., Fay, M. E., Ferris, B. G., and Speizer, F. E. (1993). *New Engl. J. Med.* 329:1753–1759.

Drewnick, F., Hings, S. S., DeCarlo, P., Jayne, J. T., Gonin, M., Fuhrer, K., Weimer, S., Jimenez, J. L., Demerjian, K. L., Borrman, S., and Worsnop, D. R. (2005). A New Time-of-Flight Aerosol Mass Spectrometer (TOF-AMS)—Instrument Description and First Field Deployment. *Aerosol Sci. Technol.* 39:637–638.

Hamilton, J. F., Webb, P. J., Lewis, A. C., Hopkins, J. R., Smith, S., and Davy, P. (2004). Partially Oxidised Organic Components in Urban Aerosol using GCXGC-TOF/MS. *Atmos. Chem. Phys.* 4:1279–1290.

Hanold, K. A., Fischer, S. M., Cornia, H., Miller, C. E., and Syage, J. A. (2004). Atmospheric Pressure Photoionization. 1. General Properties for LC/MS. *Anal. Chem.* 76:2842–2851.

Heger, H. J., Zimmermann, R., Dorfner, R., Beckmann, M., Griebel, H., Kettrup, A., and Boesl, U. (1999). On-line Emission Analysis of Polycyclic Aromatic Hydrocarbons down to pptv Concentration Levels in the Flue Gas of an Incineration Pilot Plant with a Mobile Resonance-Enhanced Multiphoton Ionization Time-of-Flight Mass Spectrometer, *Anal. Chem.* 71:46–57.

Hinz, K.-P., Kaufmann, R., and Spengler, B. (1996). Simultaneous Detection of Positive and Negative Ions from Single Airborne Particles by Real-time Laser Mass Spectrometry. *Aerosol Sci. Technol.* 24:233–242.

Intergovernmental Panel of Climate Change (IPCC). (2001). *Climate Change 2001, The Scientific Basis*. Cambridge University Press, Cambridge, UK.

Jayne, J. T., Leard, D. C., Zhang, X., Davidovits, P., Smith, K. A., Kolb, C. E., and Worsnop, D. R. (2000). *Aerosol Sci. Technol*. 33:49–70.

Jimenez, J. L., Jayne, J. T., Shi, Q., Kolb, C. E., Worsnop, D. R., Yourshaw, I., Seinfeld, J. H., Flagan, R. C., Zhang, X., Smith, K. A., Morris, J. W., and Davidovits, P. (2003), Ambient Aerosol Sampling using the Aerodyne Aerosol Mass Spectrometer. *J. Geophys. Res*. 108(D7):8425.

Kalberer, M., Paulsen, D., Sax, M., Steinbacher, M., Dommen, J., Prevot, A., S. H., Fisseha, R., Weingartner, E., Frankevich, V., Zenobi, R., and Baltensperger, U. (2004). Identification of Polymers as Major Components of Atmospheric Organic Aerosols. *Science* 303:1659–1662.

Kanakidou, M, Seinfeld, J. H., Pandis, S. N., Barnes, I., Dentener, F. J., Facchini, M. C., Van Dingenen, R., Ervens, B., Nenes, A., Nielsen, C. J., Swietlicki, E., Putaud, J. P., Balkanski, Y., Fuzzi, S., Horth, J., Moortgat, G. K., Winterhalter, R., Myhre, C. E. L., Tsigaridis, K., Vignati, E., Stephanou, E. G., and Wilson, J. (2005). Organic Aerosol and Global Climate Modeling: A Review. *Atmos. Chem. Phys*. 5:1053–1123.

Kurabuyashi, S., Yamakoshi, H., Danno, M., Sakai, S., Tsuruga, S., Futami, H., and Morii, S. (2005). VUV Single-photon Ionization Ion Trap Time-of-Flight Mass Spectrometer for On-Line, Real-Time Monitoring of Chlorinated Organic Compounds in Waste Incineration Flue Gas, *Anal. Chem*. 77:1007–1012.

LaFranchi, B. W., Zahardis, J., and Petrucci, G. (2004). Photoelectron Resonance Capture Ionization Mass Spectrometry: A Soft Ionization Source for Mass Spectrometry of Particle-Phase Organic Compounds, *Rapid Commun. Mass Spectrom*. 18:2517–2521.

McLafferty, F. W., and Turecek, F. (1993). *Interpretation of Mass Spectra*. University Science Books, Sausalito, 371 pp.

Mühlberger, Wieser, J., A. Ulrich F., and Zimmermann, R. (2002). Single Photon Ionization (SPI) via Incoherent VUV-Excimer Light: Robust and Compact Time-of-Flight Mass Spectrometer for On-Line, Real-Time Process Gas Analysis, *Anal. Chem*. 74:3790–3801.

Mühlberger, F., Zimmermann, R., and Kettrup, A. (2001). A Mobile Mass Spectrometer for Comprehensive On-Line Analysis of Trace and Bulk Components of Complex Gas Mixtures: Parallel Application of the Laser-Based Ionization Methods VUV Single-Photon Ionization, Resonant Multiphoton Ionization, and Laser-Induced Electron Impact Ionization, *Anal. Chem*. 73:3590–3604.

Mühlberger, F., Wieser, J., Morozov, A., Ulrich, A., and Zimmerman, R. (2005). Single-Photon Ionization Quadrupole Mass Spectrometry with an Electron Beam Pumped Excimer Light Source, *Anal. Chem*. 77:2218–2226.

Mühlberger, F., Streibel, T., Wieser, J., Ulrich, A., and Zimmerman, R. (2005). Single photon Ionization Time-of-Flight Mass Spectrometer with a Pulsed Electron Beam Pumped Excimer VUV Lamp for On-Line Gas Analysis: Setup and first Results on Cigarette Smoke and Human Breath, *Anal. Chem*. 77:7408–7414.

Murphy, D. M. (2005). Something in the Air, *Science* 307:1888–1890.

Murphy, D. M., and Thomson, D. S. (1995). Laser Ionization Mass Spectroscopy of Single Aerosol Particles, *Aerosol Sci. Technol*. 22:237–249.

Mysak, E. R., Wilson, K. R., Jimenez-Cruz, M., Ahmed, M., and Baer, T. (2005). Synchrotron Radiation Based Aerosol Time-of-Flight Mass Spectrometer for Organic Constituents, *Anal. Chem*. 77:5953–5960.

Nash, D. G., Liu, X. F., Mysak, E. R., and Baer, T. (2005). Aerosol Particle Mass Spectrometry with Low Photon Energy Laser Ionization, *Int. J. Mass Spectrom*. 241:89–97.

National Acid Precipitation Assessment Program (NAPAP) (1991), 1990 Integrated Assessment Report. Washington DC, The US National Acid Precipitation Program, Office of the Director.

NIST Chemistry Webbook (2005), National Institute for Standards and Technology (NIST) Standard Reference Database, Number 69, Release June 2005. Available at: http://webbook.nist.gov/chemistry/.

Noble, C. A., and Prather, K. A. (2000). *Mass Spectrom. Rev.* 19:248.

Öktem, B., Tolocka, M. P., and Johnston, M. V. (2004). On-Line Analysis of Organic Components in Fine and Ultrafine Particles by Photoionization Aerosol Mass Spectrometer, *Anal. Chem*. 76:253–261.

Rogge, W. F., Hildemann, L. M., Mazurek, M. A., Cass, G. R., and Simonelt, B. R. T. (1994). Sources of Fine Organic Aerosol. 6. Cigarette smoke in the urban atmosphere, *Environ. Sci. Technol*. 28:1375–1388

Streibel, T., Weh, J., Mitschke, S., and Zimmermann, R. (2006). Thermal Desorption/Pyrolysis Coupled with Photoionization Time-of-Flight Mass Spectrometer for the Analysis of Molecular Organic Compounds and Oligomeric and Polymeric Fractions in Urban Particulate Matter, *Anal. Chem*. 78(15):5354–5361.

Sykes, D. C, Woods III, E., Smith, G. D., Baer, T., and Miller, R. E. (2002). Thermal Vaporization-Vacuum Ultraviolet Laser Ionization Time-of-Flight Mass Spectrometer of Single Aerosol Particles, *Anal. Chem*. 74:2048–2053.

Watson, J. G. (2002). Visibility: Science and Regulation, *J. Air Waste Man. Assoc*. 52:628–713.

Wilson, K. R., Jimenez-Cruz, M., Nicholas, C., Belau, L., Leone, S. R., and Ahmed, M. (2006). Thermal Vaporization of Biological Nanoparticles: Fragment-Free VUV Photoionization Mass Spectra of Tryptophan, Phenylalanine-Glycine-Clycine and B-carotene, Submitted to *J. Phys. Chem. A* 110:2106–2113.

Woods, III, E., Smith, G. D., Dessiaterik, Y., Baer, T., and Miller, R. E. (2001). Quantitative Detection of Aromatic Compounds in Single Aerosol Particle Mass Spectrometry, *Anal. Chem*. 73:2317–2322.

Zhang, Q., Alfarra, M. R., Worsnop, D. R., Allan, J. D., Coe, H., Canagaratna, M. R., and Jimenez, J. L. (2005). Deconvolution and Quantification of Hydrocarbon-Like and Oxygenated Organic Aerosols Based on Aerosol Mass Spectrometry, *Environ. Sci. Technol*. 39:4938–4952.

Zhang, X., Smith, K. A., Worsnop, D. R., Jimenez, J., Jayne, J. T., and Kolb, C. E. (2002). A Numerical Characterization of Particle Beam Collimation by an Aerodynamic Lens-Nozzle System: Part 1. An Individual Lens or Nozzle, *Aerosol Sci. Technol*. 36:617–631.

4E.3

The chemical and physical characteristics of biomass burning particulate emissions studied at the Fire Science Laboratory. TIMOTHY B. ONASCH, Achim Trimborn, Jesse Kroll, Doug Worsnop, Ingrid Ulbrich, J. Alex Huffman, Jose Jimenez, Sonia Kreidenweis, Wei Min Hao

Biomass burning emissions may be an important contributor to secondary organic aerosol generation and the overall PM2.5 loadings in the US. Biomass burns emit significant amounts of primary particulate and gas phase compounds. However, insufficient research has focused on the volatility of these emissions, the partitioning of emitted compounds into the particulate phase, and the evolution of these emissions down wind. Biomass burns at the USDA Fire Science Laboratory are analyzed to begin to address these issues.

Controlled biomass burns were conducted in 2006 and 2007. Particulate emissions were characterized using real-time instrumentation including two WTOFAMS (electron impaction and Li ion attachment ionization), a scanning mobility particle sizer, and a thermal denuder located in front of these instruments. The high-resolution AMSs measure the nonrefractory particulate chemistry and size and enabled separation of the organic composition into oxygenated and non-oygenated components.

The fuel burned during these two studies focused on typical western and southeastern biomass that represent the major fire affected areas of the United States and were combusted in several experimental formats, including stack burns that lasted several minutes and chamber burns that were conducted inside a large room and the resulting smoke was allowed to reside inside the mixed chamber for 2-12 hours.

The biomass burns typically combusted 200 grams of material and ~80% was consumed during the flaming stage. The resulting biomass aerosol loadings varied by a factor of ~30 depending on the fuel, and the compositions varied from 50-100% organic by mass. The organic particulate emissions were dominated by the non-oxygenated components, indicating that the primary particulate emissions were not highly oxidized. Evidence for the repartitioning of the organic particulate mass from the particulate phase into the gas phase as a function of chamber dilution, transforming the particle chemistry, was observed.

4E.4

Determination of Particle-phase Organic Compounds as Wood Burning Tracers in a Residential Site of Germany. MD. AYNUL BARI, Guenter Baumbach, Bertram Kuch, Guenter Scheffknecht, Universitaet Stuttgart.

Particle-phase PM10 samples were collected with low volume sampler from November 2005 to March 2006 at a residential site surrounded by forests near Stuttgart in Germany. Samples collected on pre-baked glass fibre filters were extracted using toluene with ultrasonic bath and analysed by gas chromatograph/mass spectrometry (GC/MS). Deuterated standard compounds are added to the ambient samples prior to extraction to determine analyte recoveries in each sample. Twenty-five different organic wood smoke tracer compounds, primarily 18 species of syringol (i.e. syringaldehyde) and guaiacol derivatives which result from the pyrolysis of wood lignin, retene, resin acids (pimaric, iso-pimaric, sandarancopimaric, abietic and dehydroabietic acids) and levoglucosan, a thermal degradation product of wood cellulose were detected and quantified in 33 samples in this study. The concentrations of these compounds were compared with the fingerprints of emissions from wood combustion carried out in test facilities. It was found that the collected airborne particles contain different amounts of syringaldehyde. Syringaldehyde and other syringol and guaiacol derivatives were also found in higher amounts in particulate emissions from hardwood burning as well as ambient samples. Thus syringaldehyde seems to be an ideal tracer for particulate matter from hardwood burning. Levoglucosan was found as the most abundant organic compounds detected in all samples. The characterization of different wood smoke tracers allows to better assess the contribution of residential wood smoke to the PM10 loadings in residential sites.

Archive: Aerosol mass spectrometry: Aerosol chemical and microphysical properties

Aerosol mass spectrometry: Aerosol chemical and microphysical properties

Date:	Wednesday, October 17, 11:10 am
Symposium:	Particle Mass Spectrometry: Techniques and Applications
Topic(s):	Mass Spectrometry Environmental Instrumentation
Author(s):	Achim Trimborn (presenting) - 1 Timothy Onasch - 1 Manjula Canagaratna - 1 Jesse Kroll - 1 Dagmar Trimborn - 1 Mike Cubison - 2 Jose Jimenez - 2 John Jayne - 1 Douglas Worsnop - 1
Institution(s):	1. Aerodyne Research 2. University of Colorado
Abstract:	The Aerodyne Aerosol Mass Spectrometer (AMS) is a widely used instrument for measuring the size-resolved chemical composition of non-refractory aerosol particles. In the standard AMS, particles are flash vaporized and ionized by standard 70 eV electron impact. This \'\'hard\'\' ionization of organic molecules results in extensive fragmentation and makes it difficult to determine the molecular composition of complex mixtures. The introduction of a high resolution time of flight mass spectrometry to the AMS provides the ability to distinguish unambiguously between oxidized (secondary) and “hydrocarbon-like” (primary) aerosol. The resolution of m/Δm ~ 5000 is sufficient to resolve the elemental composition of all ions at nominal masses below m/z = 100. This allows for the quantitative determination of important chemical characteristics of the aerosol, such as the oxygen to carbon ratio of the organics. Large organic molecules generally cannot be directly measured with the AMS due to the high level of fragmentation caused by electron impact. To improve speciation of the organic aerosol, “softer” ionization methods, such as low energy electron impact (LEEI), vacuum ultra violet photo ionization (VUV) and Li ion attachment, were developed. In LEEI mode, the electron energy is reduced to ~14 eV. This results in spectra showing fragments in a higher mass range than with standard electron impact but still has significant fragmentation. VUV is softer than the LEEI approach and provides a universal ionization scheme for organic aerosols. VUV still shows significant fragmentation, though it preserves the parent ion, allowing for better speciation of the molecules. In contrast, Li ion attachment leads to almost no fragmentation of the organics, with the parent + lithium [M+6] ion exhibiting the strongest signal in the mass spectrum. While this approach is not a universal ionization technique, it is sensitive towards organics which are not highly oxidized (i.e., hydrocarbon-like aerosol). We will discuss these various ionization schemes, with a particular emphasis on the applications of Li ion attachment.
Novelty of this Contribution:	Ionization methods used in the Aerodyne AMS

Add To Schedule

< Back to Symposium

2006 Fall Meeting
Search Results

Cite abstracts as **Author(s) (2006), Title, *Eos Trans. AGU*, *87*(52), Fall Meet. Suppl., Abstract xxxxx-xx**

Your query was:
trimborn

You've chosen **one** document:

HR: 1340h
AN: **A33B-0994**
TI: First Field Deployments of an Aerodyne AMS Using Lithium Ion Attachment Ionization to Characterize Ambient Organic Aerosol Particles

AU: **Trimborn, A**
EM: *trimborn@aerodyne.com*
AF: *Aerodyne Research Inc., 45 Manning Road, Billerica, MA 01821 United States*
Jayne, J
EM: *jayne@aerodyne.com*
AF: *Aerodyne Research Inc., 45 Manning Road, Billerica, MA 01821 United States*
Northway, M
EM: *mnorthway@aerodyne.com*
AF: *Aerodyne Research Inc., 45 Manning Road, Billerica, MA 01821 United States*
Onasch, T
EM: *tonasch@aerodyne.com*
AF: *Aerodyne Research Inc., 45 Manning Road, Billerica, MA 01821 United States*
Akiama, K
EM: *kaki@jari.or.jp*
AF: *Japan Automobile Research Institute, 2530 Karima, Tsukuba, 305-0822 Japan*
Worsnop, D
EM: *dworsnop@aerodyne.com*
AF: *Aerodyne Research Inc., 45 Manning Road, Billerica, MA 01821 United States*

AB: The Aerodyne Aerosol Mass Spectrometer (AMS) is a widely used instrument to determine the size-resolved chemical composition of nonrefractory aerosol particles. In the standard AMS, particles are flash vaporized and ionized by standard 70 eV electron impact. This 'hard' ionization of organic molecules results in extensive fragmentation and makes it difficult to determine the molecular composition of complex mixtures. Previous AMS studies have been limited to classifying organics in broad categories such as "oxidized" and "hydrocarbon-like". Here we present results from the first field deployments of the Aerodyne AMS with a lithium ion ($^{6}Li^{+}$) attachment ionization source. The ionizer geometry (modified cross beam ionizer) is similar to that used in the standard electron impact version of the instrument with the Li^{+} source attached to the bottom of the original AMS ionizer cage. This setup enables the potential application of both ionization techniques. The Li ion attachment ionization scheme was successfully employed during the MCMA-2006/MILAGRO field campaign in Mexico City and the FLAME chamber study on wood burning in Missoula, Montana. Data from Mexico City show enough sensitivity to measure ambient aerosol particles with a time resolution of several minutes. Different mass spectra were observed, indicating aerosol particles from various sources. The biomass burning study results showed distinct mass spectra (i.e. molecular markers) for burns of different wood types. In particular, levoglucosan was observed and quantified. The amount of generated levoglucosan varied greatly for different biomass fuel types. The identification and quantification of specific

molecular markers by Li ion attachment and a comparison with other techniques will be presented for both studies. The results obtained from these initial field deployments represent the successful application of Li ion attachment in the Aerodyne AMS, providing a new 'soft' ionization method for the characterization of ambient organic particles.

DE: 0305 Aerosols and particles (0345, 4801, 4906)

SC: Atmospheric Sciences [A]

MN: 2006 Fall Meeting

New Search

Lithium ion attachment as a soft ionization approach for detection of organic species in the Aerodyne AMS

The Aerodyne Aerosol Mass Spectrometer (AMS) is a widely used instrument to determine the size-resolved composition of non-refractory aerosol particles. In the standard version of the instrument the particles are flash vaporized and then analyzed by electron impact ionization mass spectrometry. The ionization of organic molecules results in extensive fragmentation and makes it difficult to determine the composition for complex mixtures. Previous AMS studies have been limited to classifying organics in broad categories such as “oxidized” and “hydrocarbon-like”.

Here we present lithium ion (Li+) attachment as a new approach for determining the chemical composition of organic aerosol material with the AMS. The lithium ion source consists of an aluminosilicate/lithium oxide mixture that emits Li+ ions upon heating (~1000 °C). The ionizer geometry is identical to that used in standard electron impact version of the instrument where the Li+ source is simply attached to the original AMS ionizer. This setup provides the alternate use of both ionization techniques on the time scale of minutes.

Lithium ion attachment and electron impact ionization spectra are compared for a number of compounds including diesel soot, oleic acid, and long chain hydrocarbons. For the tested compounds the spectra show the molecular ion plus ^{6}Li as the major peak and almost no fragment ion peaks. For example, spectra of oleic acid taken using Li ion attachment consist of only one peak at m/z = 288 (oleic acid + Li6) on a linear scale. By contrast, in the case of electron impact ionization most of the ion fragments of oleic acid occur at m/z values less than 100 amu, and the molecular ion is not visible on a linear scale.
Much of the fragmentation that is observed with Li+ ion attachment results from the thermal vaporization of the aerosol particles and can be reduced by decreasing the temperature of the vaporizer. Future technical modifications for improvements to the sensitivity of this technique and results from field campaigns will be discussed.

Applying Li ion attachment to the Aerodyne AMS provides a new method for the determination of ambient organic molecules.